PRESSURE MEASUREMENTS ON JOUKOWSKY AIRFOILS IN NONUNIFORMLY SHEARED FLOWS

By

S. C. SHARMA

DEPARTMENT OF AERONAUTICAL ENGINEERING

INDIAN INSTITUTE OF TECHNOLOGY KANPUR

SEPTEMBER 1973

PRESSURE MEASUREMENTS ON JOUKOWSKY AIRFOILS IN NONUNIFORMLY SHEARED FLOWS

A Thesis Submitted
In Partial Fulfilment of the Requirements
for the Degree of
MASTER OF TECHNOLOGY

By
S. C. SHARMA

to the

DEPARTMENT OF AERONAUTICAL ENGINEERING
INDIAN INSTITUTE OF TECHNOLOGY KANPUR
SEPTEMBER 1973

CERTIFICATE

Certified that this work entitled 'PRESSURE MEASUREMENTS ON JOUKOWSKY AIRFOILS IN NONUNIFORMLY SHEARED FLOWS' by S.C. Sharma has been carried out under my supervision and that this has not been submitted elsewhere for a degree.

A. K. Gupta

(A.K. Gupta)
Assistant Professor
Department of Aeronautical Engineering
Indian Institute of Technology, Kanpur

ACKNOWLEDGEMENT

I am very grateful to Dr. A.K. Gupta, who guided and encouraged me at all stages of the work. He has been a real source of inspiration and it was a pleasure to work under him.

I want to express my thanks to Shri R. Krishnamurthy, who took lot of pains during the workshop job.

I want to thank Shri K.S. Muddappa, who helped me during the Experimental Program.

Thanks are also due to my friends who helped me during the last stage of the work.

In the end, I thank Mr. Kumar for his excellent typing.

ABSTRACT

An experimental study of a two-dimensional cambered Joukowsky airfoil (chord 15 cms, thickness 15% and camber 10%.) has been carried out in nonuniformly sheared flows. The pressure distribution over the airfoil has been measured to compute the aerodynamic coefficients, C_L and C_M for various angles of attack and at different vertical locations, to observe the effect of the interaction of stream shear, camber and thickness on the airfoil characteristics. Earlier work showed that under similar flow conditions, the maximum lift on a two-dimensional symmetrical Joukowsky airfoil increased when it was located slightly below the flow centre line. The present results for symmetrical airfoil show good agreement with the previous work. In addition the results for cambered Joukowsky airfoil immersed in nonuniformly shear flow show an increase in the lift in agreement with the theoretical predictions.

CONTENTS

LIST OF SYMBOLS

X, Y, Z	Cartesian Co-ordinates
c	Airfoil Chord
t	Maximum Thickness of the Airfoil
h	Test-section Height
b	Span of the Test-section
h'	Distance from the Tunnel Centre-line to the Slip-stream Boundary
y	Vertical Location of the Airfoil Mid-chord
$\bar{U}$	Local Mean Velocity
$\tilde{U}$	Average Velocity in the Slip-stream
$\underline{U}$	Uniform Velocity of the Simulated Free-stream
U_o	Uniform Free-stream Velocity
U_{max}	Velocity at the Slip-stream Boundary
U_{min}	Velocity at the Centre of the Slip-stream
K	Shear Parameter ... Eq. 1.1
q	Shear Parameter ... Eq. 1.4
K_o	Screen Resistance Coefficient ... Eq. 1.7
p_s	Static Pressure on the Airfoil Surface
p_∞	Free-stream Static Pressure
ρ	Density of Air
$\bar{C}_p$	Uniform Flow Pressure Coefficient, $\frac{p_s - p_\infty}{\frac{1}{2}\rho U_o^2}$
C_L	Lift Coefficient, Based on the Airfoil Mid-Chord Dynamic Head
$\bar{C}_L$	Lift Coefficient Based on the Stagnation Stream-line Dynamic Head

C_p	Nonuniform flow pressure coefficient $\frac{p_s - p_\infty}{\frac{1}{2}\rho \bar{U}^2}$
C_D	Drag Coefficient Based on the Airfoil Mid-chord Dynamic Head
C_M	Pitching Moment Coefficient Based on Airfoil Mid-Chord Dynamic Head
C_N	Normal Force Coefficient
C_c	Chord-wise Force Coefficient
τ	Thickness Ratio = t/c
α	Angle of Attack
$\bar{\alpha}$	$\alpha - \alpha_o$
d	Diameter of Rod
s	Spacing Between the Rods
σ	Solidity of the Screen, $\frac{d}{s}$
β	Defined in Eq. 1.8
u'	Mean Fluctuating Velocity in X Direction

Subscripts

u	Upper Surface
l	Lower Surface

LIST OF FIGURES

Figure

LIST OF PLATES

CHAPTER 1

INTRODUCTION

In the study of flow over wings, the free-stream velocity profile is taken to be uniform. But there are certain situations when the free-stream flow is not uniform, or we can say it has velocity gradients or shear, as in the case of a propeller airplane where part of the wing is sumberged in the slip-stream. The local lift coefficient on this part of the wing may differ from that on the rest of the wing, changing the span wise lift distribution accordingly. Though this problem of the influence of stream non-uniformities on the airfoil characteristics is not new, yet the attention given to it has not been persistent. One approach of simplification in this regard has been to replace the shear slip-stream with an effective uniform jet, free of all gradients having a momentum flux equal to the average of that in the shear slip-stream. In this approach a general assumption is that the flow nonuniformities or shear has no significant influence on the airfoil characteristics.

Recently the study of the interaction between a propeller slip-stream and a wing has become important since the existence of strong gradients of the longitudinal velocity in the slip-stream seems to change the airfoil characteristics considerably in a favourable manner. An understanding of the maximum lift behaviour of the airfoils in non-uniformly sheared flow should enable the

airplane designer to take the maximum advantage of this. This knowledge can be made use of in the field of V/STOL aircraft with highly flapped wings immersed in a highly sheared slip-stream.

1.1 Review of the Previous Work

a. Airfoils in Nonuniform Flow

In one of the earliest works Tsien[1] (1943) considered a symmetric Joukowsky airfoil in an infinite inviscid stream with a uniform shear K, defined as

$$U = U_o \left(1 + K \frac{y}{c}\right) \tag{1.1}$$

An exact solution for the aerodynamic forces was obtained predicting an increase in the lift coefficient due to the thickness-shear interaction. Sowyrda[2] (1958) extended this theory for cambered Joukowsky airfoils mainly due to his interest in the deflected shear slip-stream over highly flapped wing configuration of V/STOL aircraft. His results for lift coefficient and the pitching moment coefficient to the first order in the thickness and camber are

$$C_L \approx \left[1 + \tau + \frac{\tau K^2}{32}\right] 2\pi\alpha + 2\pi \left[\frac{\tau K}{4} + \frac{2\bar{h}}{c}\left(1 + \frac{K^2}{32}\right)\right] \tag{1.2}$$

$$C_{M_{c/2}} \approx \left[1 + \tau + \frac{\tau K^2}{16}\right] \frac{\pi}{2}\alpha + \frac{\tau \pi K}{64} \tag{1.3}$$

where $\bar{h}$ is the maximum height of the airfoil camber line. If in Eq. 1.2, $\bar{h}$ is put equal to zero, the value of C_L given by Tsien's theory is obtained.

Jones[3] (1957) investigated the effect of nonuniform flow on airfoil characteristics with a parabolic velocity distribution given by

$$U = U_1 \left[1 + 8q \left(\frac{y}{c}\right)^2 \right] \qquad (1.4)$$

His results for C_L and $C_{M_{c/2}}$ to the first order in α and q (y/c) are given by

$$C_L \approx 2\pi \left[(1 + 1.11q)\,\alpha + \frac{2\bar{h}}{c} \right] \qquad (1.5)$$

$$C_{M_{c/2}} \approx \frac{\pi}{2}\,\alpha \left[1 + .866\,q \right] \qquad (1.6)$$

A systematic research programme was initiated at the Cornell Aeronautical Laboratory* Inc. Buffalo, N.Y. to investigate the effect of nonuniformly sheared slipstream on airfoils. Sowyrda's work[2] was the earliest in this context. Vidal et.al[4] (1960) made experimental measurements by simulating a two-dimensional non-uniform slip-stream in a wind tunnel and carried out tests on a 17% thick symmetrical Joukowsky airfoil. The airfoil section was chosen to verify the experimental results with the known theories[1-3]. It was reported that the maximum lift available changed markedly when the airfoil was positioned slightly below or above the flow centre line Vidal[5] (1962) found that the stalling characteristics of airfoils in shear flows depended upon the product of the local shear and its derivative, which when negative, delayed stalling and promoted it when positive.

---

* now CALSPAN

The airfoil model used in all these cases was provided with a strain gauge balance which provided force data. The unusual maximum lift behaviour called for a knowledge of the pressure distribution study over the airfoil surface. Ludwig and Erickson[6] (1971) carried out such tests in a nonuniformly sheared slip-stream, over a 17% thick symmetrical Joukowsky airfoil with static pressure tappings on its surface. The aerodynamic coefficients were computed from the pressure distribution. For theoretical predictions they extended a computer program due to Brady and Ludwig (1966)[6] (Ref.6) to include nonuniform slip-stream boundaries as discontinuities. Their pressure measurements showed that the change in stalling characteristics in a nonuniformly sheared flow was due to change in the upper surface pressure distribution. Near the flow centre line the lift characteristics become independent of the shear when stagnation stream line dynamic pressure was used for computing the lift coefficient.

b. Production of Nonuniform Shear Flow

The production of nonuniform shear flow is very much essential for an experimental study of airfoils in such flows. This type of flow can be generated in a wind tunnel, by incorporating variable losses in the test section. These losses can be produced by placing an array of span wise rods/wires with variable spacings.

When a turbulent stream of fluid passes through a wire gauge, it becomes less turbulent and the steady disturbances are reduced in intensity. The gauze offers a resistance to the component

of flow normal to its plane. If a pressure difference p_1-p_2 is required to drive fluid of density ρ, through a wire gauze at a velocity U, the drag coefficient K_o (hereafter called screen resistance coefficient), is given by

$$K_o = \frac{p_1-p_2}{\frac{1}{2}\rho U^2} \tag{1.7}$$

Taylor and Batchelor[7] (1949) solved the problem of flow through a gauze and found that the longitudinal velocity was altered in the ratio

$$\frac{u_2}{u_1} = \frac{1+\beta-\beta K_o}{1+\beta+K_o} \tag{1.8}$$

where $\beta = 1.1\ (1+K_o)^{-1/2}$, and the flow patterns far downstream were not the same as those far upstream.

Owen and Zienkiewicz[8] (1957) found a linear relationship between downstream velocity distribution and K_o, the screen resistance coefficient, distribution across a grid of horizontal wires. By inserting such grid in the test section of a wind tunnel, a weak uniform shear flow was obtained. Elders[9] (1958) obtained similar results. McCarthy[10] (1964) obtained a nonlinear relation between downstream velocity distribution and K_o for three dimensional highly nonuniform flows. Three different types of screens were tested to establish the validity of the results. Vidal et.al[4] (1960) extended Owen and Zienkiewicz's method[9] to produce a highly nonuniform shear stream. For experimental results, empirical formulas with trials and errors along with the theory were

used. The velocity profiles of Vidal et.al[4] were in good agreement with the theory.

Kotnasky[11] (1966) made use of a honey comb structure for generating nonuniform flows. This celluler structure of honey comb eliminates most of the support and structural problems associated with shear screens of rods and wires. Because of the built-in straightness, the flow downstream was relatively homogeneous. Recently, Livesay and Laws[12] (1973) have given a method of generating axisymmetric gauze screens required to produce desired velocity profiles by developing and adding corrections to Elder's (1958) theory[9].

1.2 The Present Work

The present work is experimental and is an extension of the work of Ludwig and Erickson[6] (1971), in which a 2-D, 17% thick symmetrical Joukowsky airfoil was tested for pressure distribution in a simulated propeller slip-stream. In the present experiments a 2-D Joukowsky airfoil of 15 cms.chord with 10% camber and 15% thickness was tested in a nonuniformly sheared flow to record the pressure distribution along the mid-span. The objective was to study the effect of camber on the airfoil characteristics for different angles of attack and at different vertical locations.

A nonuniformly sheared flow similar to, but with a lower value of the shear parameter than in Ref.6 was obtained by introducing variable losses in the wind tunnel test section with the

help of a shear screen. This screen consisted of an array of rods arranged horizontally. Mean flow characteristics including the turbulence level of the nonuniform shear flow were measured.

A symmetrical Joukowsky airfoil (15% thickness and 15 cm. chord) was also tested in uniform and nonuniformly sheared flow in order to compare results with the previous investigations.

Lift characteristics for each airfoil were computed from the pressure distribution recorded. An attempt to investigate the stalling characteristics of the two airfoils was also made.

CHAPTER 2

EXPERIMENTAL PROGRAM

The testing of two 2-D Joukowsky airfoils (cambered and symmetrical) was carried out in a nonuniform sheared flow, for various angles of attack at different vertical locations. The nonuniform shear flow was produced by incorporating variable losses with the help of a screen consisting of an array of horizontal rods of varying diameters and spacings, and mounted in the test section. These spacings and diameters could be varied to produce desired type of shear flow. The airfoil was mounted on a simple support which permitted an independent change of the angle of attack and the vertical location (Plate No.3).

2.1 Equipment

(i) Wind Tunnel:

The experiments were conducted in the 2-D test-section of the low speed wind tunnel in the Aero. Lab. at I.I.T. Kanpur. This tunnel has a special feature that with a common blower section, two different test-sections can be used one at a time (Fig.1). The 2-D test-section with a contraction ratio of 9.5 has a X-section of 1'x4' and a length (distance between the contraction cone and the diffuser) of 5'-6". The maximum velocity attained with no model in it is 180 fps and the turbulence level at this speed is 1.4% .

(ii) Airfoil Models:

Two Joukowsky airfoils (cambered and symmetrical) (Plates 1a,b) were used for the testing. Both the airfoil models were 15% thick, having chord of 15 cms and span of 12". These were manufactured in the Aero. Workshop out of compressed wood. There were twenty five static pressure tappings along the mid-span of the symmetrical airfoil as shown in Fig. 2b, and twenty three static pressure tappings along the mid-span of the 10% camber airfoil, as shown in Fig. 2a. The copper tubes of 1/16" dia., used as pressure leads from both the models, were taken out from one side of the airfoil model through a hole of 1/2" dia. at the mid-chord. One M.S. tube of 3/4" O.D with outside threads was fixed permanently (Plates 1a,b) for the model support as well as for taking the pressure leads to the multitube manometer. The pressure measurements at the trailing edge were taken with the help of two static pressure probes as it can be seen from the airfoil cross-section (Figs. 2a,b) that taking the pressure leads out of the trailing edge was not possible.

(iii) Model Support:

Two wooden planks (Plate 2) were manufactured in the Aero. Workshop which served the purpose of holding the models. Seven different vertical locations each 3/4" apart, were marked out between the two planks. At these locations, holes of 3/4" dia. were drilled and 1/32" brass bushes were pushed tight. The 1/16" collar of the bush served the purpose of washer for the hexagonal

nut which was used for fixing the model. Seven holes were made on the wind tunnel wall and the model rested on a hinged support and could rotate about its mid-chord point. The angle of attack was read on a protractor (which could be easily removed), with the help of a sharp, brass indicator (Plate 3). The indicator could be easily slipped on to the threaded M.S. tube and tightened.

(iv) Screens for Nonuniform Shear Flow:

Two different screens (Plates 4a,b) were used for producing two different nonuniform shear flows. The screens consisted of Aluminium rods of diameters 1/4" and 1/2" with varying spacings. The array of rods arranged horizontally was firmly secured in a wooden frame of size 1'x4'. The corners of the frame were properly rounded off to make them streamlined. The screen was placed (Fig.3) in the test-section 20" downstream of the contraction cone and the airfoil was placed 38" further downstream. This distance was the same as suggested by Ludwig and Erickson[6] (1971). The screen was held against six aluminium supports of L section, which were firmly screwed to the tunnel walls (Plate 5).

The main criterion of the shear screen design was the proper distribution of the screen resistance coefficient K_o, given by

$$K_o = \frac{p_1 - p_2}{\frac{1}{2}\rho U^2} \qquad (1.7)$$

The distribution of the solidity over the range was determined by using one of the following empirical relations[4]:

$$K_o = \left(\frac{\sigma}{1-\sigma}\right)^2 \qquad (2.1)$$

$$K_o = \frac{\sigma - 2/3\sigma^2}{(1-\sigma)^2} \qquad (2.2)$$

The second relation was used because it agreed well for data with low solidities[4]. By choosing proper rod/wire size, spacings could be found out. It was observed in the present work that the spacings needed modifications near the centre line and near the wall. In fact, the screen no.2 was a modification of screen no.1 to obtain the desired linear velocity profile near the centre, as shown by the Fig. 4c.

(v) Instrumentation and Accessories:

(i) Hot Wire Anemometer:

A DISA, Model 55A01, Constant Temperature Hot Wire Anemometer was used for the turbulence measurements. A single hot wire proble, normal to the flow was traversed in the y-direction from the centre of the tunnel test section at the point of airfoil mid-chord location. A Tektronix Type 545B Oscilloscope was used for monitoring the hot-wire signals.

(ii) Multitube Manometer:

This multitube manometer using water as the working fluid, has a set of one hundred tubes and can be inclined at any desired angle. There is a freezing arrangement available for arresting the pressure records.

2.2 Procedure

The first part of the Experimental Programme was the study of mean flow characteristics. The measurements included the uniform free-stream profile and turbulence measurements. This was repeated with both the screens. The existing Pitot-comb with 40 tubes spaced 1.9 cms. apart was extensively used for the mean velocity profile measurements. It was observed that the velocity profile in all the cases was satisfactorily symmetrical about the flow centre line. In the final calibrations, a 3/8" Pitot-static tube was traversed in the upper half only. Similarly the hot wire probe was also traversed in the upper half. The span wise velocity profile was measured with the help of a horizontal Pitot comb, mounted on the vertical Pitot comb (Plate 6).

The second part consisted of taking the pressure distribution data on both the airfoils in uniform and nonuniform flows, for different angles of attack and in case of nonuniform flows for different vertical locations. The multitube manometer inclination was kept at 30° with the vertical for these measurements.

2.3 Data Reduction

The static pressure measurements on the airfoil surface were reduced to the form of aerodynamic coefficients[13], C_N and C_c, by performing the integration of pressure coefficient along the X and Y co-ordinates

$$C_N = - \int_0^1 (C_{p_u} - C_{p_L}) \, d\, x/c \qquad (2.3)$$

$$C_c = \oint C_p \, d\, y/c \tag{2.4}$$

$$C_L = C_N \cos\alpha - C_c \sin\alpha \tag{2.5}$$

$$C_D = C_N \sin\alpha + C_c \cos\alpha \tag{2.6}$$

where α is the angle of attack.

The pitching moment about the leading edge is given by

$$C_{M_{LE}} = \int_0^1 \Delta C_p \, x/c \, d\, x/c + \oint \Delta C_p \, y/c \, d\, y/c \tag{2.7}$$

where nose up pitching moments are positive. Normally these integrations are performed graphically. In the present work, these integrations were performed numerically (Appendix A-2b) on IBM 7044/1401 Computer, installed at IIT/K Computer Centre.

CHAPTER 3

EXPERIMENTAL RESULTS

3.1 Mean Flow Characteristics

a. Uniform Flow

Fig. 4a presents the mean velocity profile at the airfoil mid-chord location, for different speeds plotted in the dimensionless form, U/U_o vs y/h_2. It shows that there is a variation of $\pm$ 2.0% and $\pm$ 0.5% at the nominal wind speeds of 134 fps and 164 fps respectively.

b. Nonuniformly Sheared Flows

Two different velocity profiles were obtained, using two different screens (Plates 4a,b). Fig. 4b shows the mean velocity profile with the screen no.1, having a shear parameter q=0.248. The pitot-comb readings have also been plotted on the same scale to establish the symmetry of the flow about its centre line. The velocity profile at the flow centre line has a Reynolds no. (based on the airfoil chord) of 2.63×10^5* at 7" above and below the flow centre line. The velocity profile upto this point is parabolic in nature. The variation of the turbulence level is plotted on the same scale. It is observed that the maximum turbulence is observed when slip-stream boundary and the simulated free-stream mixing takes place, which is consistent with the highly unstable nature of the discontinuous flows. The magnitudes of $\underline{U}/\tilde{U}$ and $U_{min}/\tilde{U}$ would be equal for a nonuniformly sheared flow simulating a two dimensional propeller slip-stream.

* and varies upto 3.56×10^5

Fig. 4c shows the mean velocity profile with a shear parameter of K = 0.34. The Reynolds no. in this case varies from 2.32×10^5 at the flow centre line to 3.25×10^5 at 6.8" above and below the same. This portion has a uniform shear. A higher turbulence level is observed, because of the higher solidity of the screen (Plate 4b). The magnitude of $\underline{U}$ is less than that of $U_{min.}$ which seems satisfactory for lower value of the shear parameter.

Fig. 4d shows a comparison of the two nonuniform shear flows with the design shear flow. The reasons and limitations for this are discussed in the Appendix. Fig. 4e presents the span wise velocity profile, at the flow centre line ($y/\frac{h}{2} = 0$). Despite fluctuations and nonuniformity of the flow near the walls, the flow within 1.0" on either side of the centre (pressure tap locations) is uniform within a few percent or less.

3.2 Pressure Distribution Over the Airfoils

A large number of pressure distributions were recorded over the two airfoils for different angles of attack and seven vertical locations. In this chapter, however, the pressure distribution plots have been presented for only two vertical locations, just below and above the flow centre line.

The pressure coefficient C_p is based on the mid-chord dynamic pressure, at that particular y-location. With a change in angle of attack, the stagnation stream line changes and so does

the dynamic pressure. It has been suggested[6] that the dynamic pressure of the stagnation stream line be used for computing the aerodynamic coefficients. Since the exact location of the stagnation stream line was difficult to determine, Ludwig and Erickson[6] used the difference between the free-stream static pressure and the maximum magnitude of the static pressure on the leading edge portion of the airfoil, as the stagnation stream-line dynamic pressure. The lift coefficients have been computed using the stagnation point dynamic pressure obtained in this manner, as well as using the mid-chord dynamic pressure.

The dotted line shown in the C_p vs x/c plots indicate the pressures obtained by traversing a two prong static probe in the viscinity (within 1") of the trailing edge.

a. Symmetrical Airfoil:

(i) Uniform Flow

Fig.5 shows the C_p vs x/c plot at a Reynolds no. of 3.19×10^5. The suction peak rises with the increase in angle of attack. At $\alpha = 14.5^\circ$, complete stalling is observed.

(ii) Nonuniformly Sheared Flow

Fig. 6a presents the C_p vs x/c plot in a nonuniformly sheared flow, with q=0.248, and the airfoil located just below the flow centre line. A rise in the suction peak is observed as compared with that in the uniform flow. Even at $\alpha = 16.0^\circ$, the stalling is not observed. Fig. 6b shows the similar plot for the airfoil location just above the flow centre line. A comparison

of the two figures (6a,b) does not show any marked difference in the pressure distribution.

Figs. 7a and 7b are the pressure plots in a nonuniformly sheared flow with K=0.34, at $y/h' = -.11$ and $y/h' = 0.11$ respectively. A marked difference can be observed between the two plots. At $y/h' = -0.11$, the suction peak for $\alpha = 16^{\circ}$, is higher than that at $y/h' = 0.11$. A comparison of Fig. 7b with Fig.6b shows that the suction peak with K = 0.34 is still higher than that with q = 0.248. Fig. 7c shows a comparison of the pressure distribution over symmetrical airfoil with that from Ref.6. Though the shear is not the same in the two cases, there seems to be a good agreement.

b. Cambered Airfoil:

(i) Uniform Flow

Fig.8 shows the pressure distribution plot for the cambered airfoil. Unlike that in the symmetrical airfoil, the maximum suction is observed in this case near the quarter-chord point. As the angle of attack increases there is an increasing droop in the C_p vs x/c curve around $x/c \approx 0.10$. The suction peak again rises upto $x/c \approx 0.25$, and thereafter gradually falls towards the trailing edge. At higher α's, there is a larger drop in C_p. Laminar separation bubbles[15] can cause such upper surface pressure distributions over airfoils.

(ii) Nonuniform Flow:

Figs. 9a and 9b show the pressure distribution plots with q = 0.248, at $y/h' = -0.107$ and $y/h' = 0.107$ respectively. A

comparison of Figs. (9a,b) with Fig.8 does not show any appreciable difference between the pressure distributions in these two cases. Figs. 10a and 10b show considerable increase in the suction over the upper surface. However, the trend of the C_p vs x/c curve is the same as in Fig. 8.

CHAPTER 4

DISCUSSION

Tsien's analysis[1] has shown that flow patterns over a circular cylinder in uniform shear flow are different than those in the uniform flow, implying a corresponding change in the aerodynamic coefficients. Other investigators (Ref.2-6) have subsequently found that the lift, drag and moments are markedly different in nonuniform flow from those in uniform flow. In particular Ludwig and Erickson[6] (1971) have concluded that the change in lift is mainly due to the upper surface pressure distribution. The present results, in general, are in fair agreement with these previous observations.

4.1 Effect of Stream Shear

Pressure distributions over symmetrical airfoil, as shown in Figs. 5-7, indicate that nonuniform stream shear brings about a change in the suction pressure on the upper surface. Accordingly, a change in the lift coefficient is also observed in Figs.15a, b and c, where lift coefficient for symmetrical airfoil is plotted as a function of the angle of attack for different shears. A study of the lower surface pressure distribution in Figs. 5-7, on the other hand shows no significant change due to stream shear.

Ludwig and Erickson[6] have shown that the lift characteristics of symmetrical Joukowsky airfoil become independent of stream shear when the lift coefficient is normalised with the stagnation

stream line dynamic pressure in place of the mid-chord dynamic pressure. This is confirmed in the present experiments as shown in Fig. 15c.

The pressure distribution over the cambered airfoil (Figs. 8-10) also shows a rise in the suction pressure over the upper surface, in nonuniform shear flow thereby improving the lift characteristics (Fig.16b) in this case also. Fig. 16c shows $\bar{C}_L$ and $\underline{\alpha}$ plot for the cambered airfoil where $\bar{C}_L$ is the lift coefficient based on stagnation stream line dynamic pressure and $\underline{\alpha} = \alpha - \alpha_{U_o}$, where α_{U_o}, is the angle of attack for cambered airfoil in non-uniform flow at which the lift coefficient is the same as that of the cambered airfoil at zero angle of attack in uniform flow. It is observed that the lift coefficient again becomes independent of the stream shear.

McCullough and Gault[14] have classified three different types of stalls:

1. Trailing Edge Stall: The separation point of the turbulent boundary layer moves towards the leading edge as the incidence increases.

2. Leading Edge Stall: Where abrupt separation of the laminar boundary layer takes place near the leading edge without further reattachment.

3. Thin Airfoil Stall: Where a laminar separation takes place near the leading edge followed by turbulent reattachment at a point which moves towards the trailing edge with the increase in the angle of attack.

Of these categories of stall, the last one is termed due to laminar separation bubble formation[15] which is possible for a certain range of Reynolds no., which further depends upon the pressure distribution, the surface curvature, the surface roughness and the turbulence of the free-stream[15]. A Table summarising the stalling characteristics of the two Joukowsky airfoils under different flow conditions has been prepared and presented below:

TABLE

Airfoil	Shear	y/h'	u'/$\bar{U}$ %	Stalling angle	Type of stall	Figure
Symmetrical	K=0	0	1.65	13°	Leading Edge Stall	15a
	q=0.248	.107	2.8	16.5°	" " "	15b
	q=0.248	-.107	2.8	16°	" " "	15b
	K=0.34	.11	3.1	14°	" " "	15b
	K=0.34	-.11	3.1	16.5°	" " "	15b
Cambered	K=0	0	1.65	10°	Thin Airfoil Stall	16a
	q=0.248	.107	2.8	14°	" " "	16b
	q=0.248	-.107	2.8	12°	" " "	16b
	K=0.34	.11	3.1	13°	" " "	16b
	K=0.34	+.11	3.1	13°	" " "	16b

In Figs. 15-16, a difference in the lift characteristics is observed for q=0.248 and K=0.34. This difference is due to a change in the stream shear which alters the pressure distribution (Figs. 13a and b) over the upper surface of the airfoil. Figs.15d and 16d present the positive stalling moments at leading edge as a

function of pitch angle in the nonuniform shear flow. When compared with the uniform flow pitching moment (Figs.15a and 16a) a large increase is observed. For the sake of comparison dotted lines present the theoretical curves due to Sowyrda[2] in uniform shear flow.

4.2 Effect of Vertical Location

It has been shown[6] that slightly below the flow centre-line, an increase in the lift was observed. The present results show good agreement with this. Fig. 15b for symmetrical airfoil shows that for $y/h' = .11$, and $K=0.34$, the magnitude of $C_{L_{max}}$ is 1.46, whereas for $y/h' = .11$ it is 1.26. The stalling angle has increased from 14° in case of $y/h' = .11$ to around 16.5° at $y/h' = -.11$, while with $q = 0.248$, the two values of $C_{L_{max}}$ being close, no such inference could be made. In Fig. 16b for cambered airfoil at $y/h' = -.11$ and $y/h' = .11$, for $K = 0.34$, the value of $C_{L_{max}}$ is more in the former case than that in the latter case, the stalling angle is close to 13° in these two cases. Whereas with $q = 0.248$, the $C_{L_{max}}$ is more at $y/h' = -.11$ than that at $y/h' = .11$, the stalling angle is higher at the latter location.

Figs. 11-12 show the pressure plots for symmetrical and cambered airfoils at all the seven different vertical locations used. It is observed that near the slip-stream boundaries, there is a decrease in the $C_{L_{max}}$. It can be remarked that the regions of importance in the nonuniform shear flows simulating 2-D

propeller slip-stream lies near the flow centre line. Figs.19a, b show the lift curve at the remaining vertical locations for the symmetrical and cambered Joukowsky airfoils in nonuniform shear flow with K=0.34.

4.3 Effect of Camber

Figs. 14a and b show the effect of camber on the pressure distribution over the airfoil with q=0.248 and K=0.34 respectively. Fig. 17 shows the plot of $C_L - C_{L_{K=0}}$ against angle of attack, for the symmetrical and cambered airfoil. It is observed that the increment in lift is more in the case of cambered airfoil whereas the stalling is delayed to higher angles in the case of symmetrical airfoils. It can be seen from Figs. 15d and 16d that camber has no significant effect on the stalling moment.

4.4 Conclusion

In view of the present work, it is concluded that

1. The lift characteristics of the cambered airfoil are also improved in the nonuniformly sheared flow, near the flow centre-line.
2. The cambered airfoil gives nearly two-fold increment in lift over the symmetrical airfoil, whereas stalling is delayed to higher angles in case of symmetrical airfoils as compared with that in cambered airfoil.

3. Thin airfoil stall occurs in case of cambered airfoil near the flow centre-line in the nonuniformly sheared flow and leading edge stall occurs in case of symmetrical airfoil.

4. When the lift coefficient is based on the stagnation streamline dynamic pressure, the stalling characteristics as indicated by $\bar{C}_L$ vs α curve seems to change.

4.5 Further Suggestions

1. The computer program due to Ludwig and Erickson[6] for symmetrical airfoil in nonuniformly sheared flow should be extended to cambered airfoil.
2. Oil film studies to visualize the boundary layer separation should be made.
3. Screens producing highly sheared nonuniform flows should be used for carrying out further experiments.
4. Pitch angle measurements of the flow should be made to correct the angle of attack.
5. The discrepency in the theoretical curve and measured value of C_L in Figs. (15a and 16a) can probably be reduced by making careful measurements of the static pressure.

REFERENCES

1. Tsien, H.S., 'Symmetrical Joukowsky Airfoils in Shear Flow'. Quart. App. Maths., Vol. 1, pp 130-148, 1943.

2. Sowyrda, A., 'Theory of Cambered Juokowsky Airfoils in Shear Flow'. Cornell Aeronautical Laboratory Report No. AI-1190-A-2, September 1958.

3. Jones, E.E., 'The Forces On a Thin Airfoil in Slightly Parabolic Shear Flow'. Z.A.M.M., Vol. 37, No.9-10, pp 362-370, 1957.

4. Vidal, R.J., Hilton, J.H., and Curtis, J.T., 'The Two Dimensional Effects of Slip-stream Shear On Airfoil Characteristics'. Cornell Aeronautical Laboratory Report No. AI-1190-A-5, September 1960.

5. Vidal, R.J., 'The Influence of Two Dimensional Stream Shear on Airfoil Maximum Lift'. Journal of Aero-Space Sciences, Vol. 29, No.8, pp 889-904, 1962.

6. Ludwig, G.R., and Erickson, J.C. Jr., 'Airfoils in Two Dimensional Non-Uniformly Sheared Slipstream'. Journal of Aircraft, Vol.8, No.11, pp 874-880, November 1971.

7. Taylors, G.I. and Batchelor, G.K., 'The Influence of Wire Gauze on Small Disturbances in Uniform Stream'. Quart. Jour. Mech. and App. Maths., Vol. II, Pt.1, pp 1-29, 1949.

8. Owen, P.R. and Zienkiewicz, H.K., 'The Production of Uniform Shear Flow in a Wind Tunnel'. Jour. Fluid Mech., Vol.2, Pt.6, pp 521-531, August 1957.

9. Elders, J.W., 'Steady Flow Through Nonuniform Gauges of Arbitrary Shapes'. Jour. Fluid Mech. Vol. 5, pp 355-68, 1968.

10. McCarthy, J.H., 'Steady Flow Past Nonuniform Wire Grids'. Jour. Fluid Mech., Vol. 19, pp 491-512, 1964.

11. Kotnasky, D.R., 'The Use of Honey Comb for Shear Flow Generation'. A.I.A.A. Journal, Vol. 4, No.8, pp 1490-91, 1966.

12. Livesay, J.L. and Laws, E.M., 'Simulation of Velocity Profiles by Shaped Gauze Screens', A.I.A.A.Journal, Vol.11, No.2,p184, Feb. 1973.

13. Pankhrust, R.C. and Holders, D.W., 'Wind Tunnel Techniques'. PITMAN, London.

14. McCullough, G.B. and Gault, D.E., 'Examples of Three Representative Types of Airfoil-section Stall at Low Speeds', NACA TN 2502.

15. Tani, A., 'Low Speed Flows Involving Bubble Separation'. Progress in Aeronautical Sciences, Vol. 5, No.2, Pergamon Press, 1964.

16. Houghton, E.L. and Brock, A.E., 'Aerodynamics for Engineering Students', Edward Arnold Ltd., London, 1966.

1_2_D TEST SECTION 5'-6" x 1' x 4'
2_3D TEST SECTION 5'-6" x 3' x 2'
3_CONTRACTION CONE
4_DIFFUSER
5_CENTRAL DIFFUSER
6_BLOWER SECTION (2_12 BLADED, 15 HP FANS)
7_TURNING VANES
8_SCREENS
T_TURNING BOX

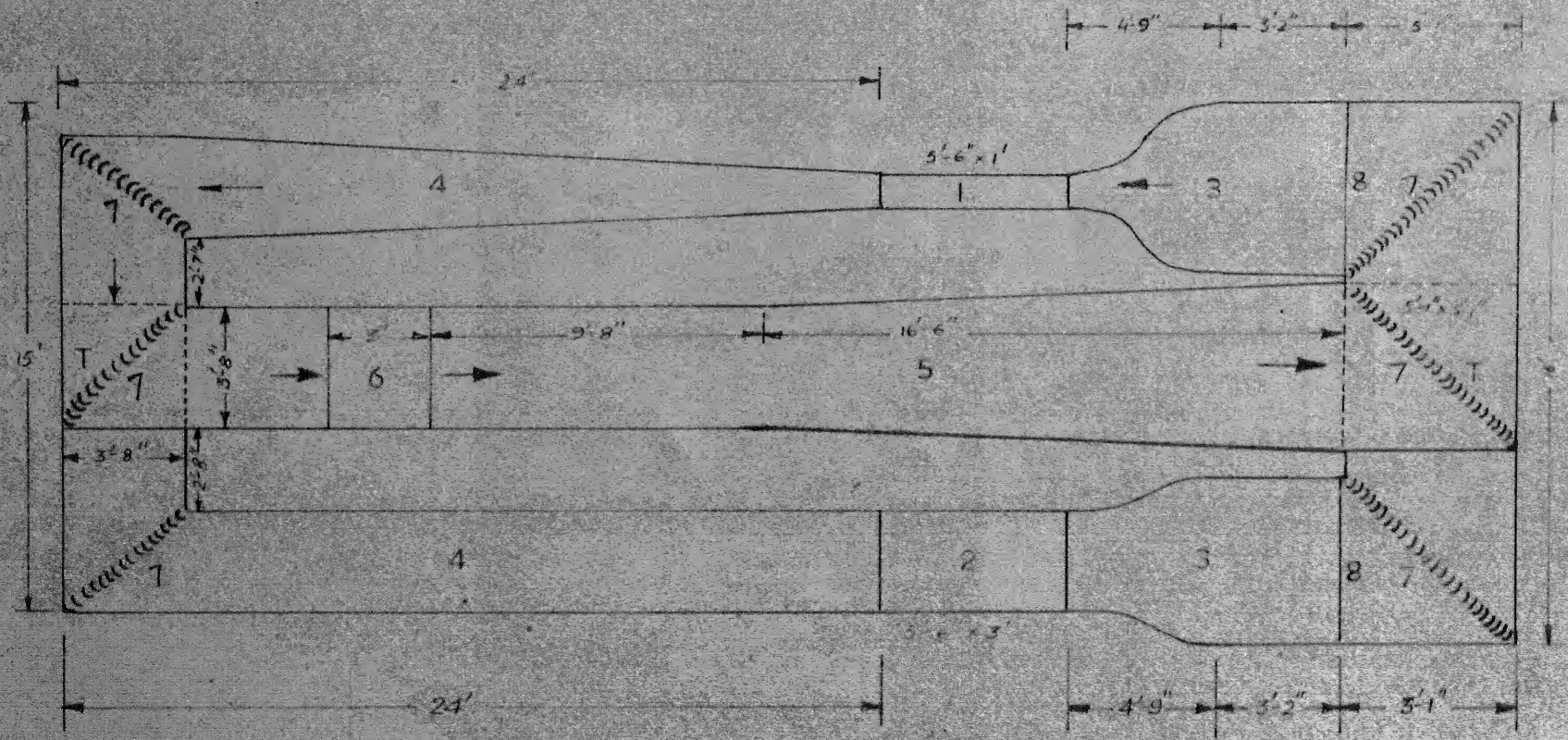

FIG.1_PLAN OF WIND TUNNEL IN THE AERO LAB. IIT/K

SCALE_HALF FULL SIZE - ONE CM. TO ONE FOOT

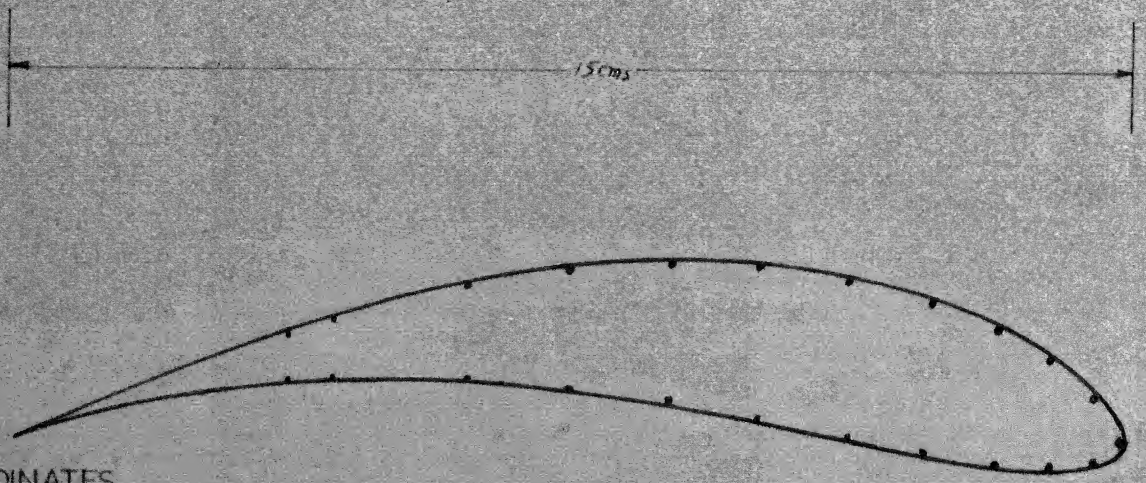

AIRFOIL CO-ORDINATES

X(cms)	Y_U(cms)	Y_L(cms)
0	0(LE)	0
0·114	0·5440	-·2530
0·452	0·7500	-·3990
1·005	0·8830	-·4330
1·755	1·0030	-·3630
2·679	1·0730	-·2700
3·750	2·2500	0·000
4·955	2·4170	·2320
6·298	2·4560	·4540
7·500	2·3660	·6340
8·802	2·1600	·7500
10·065	1·8600	·7830
11·250	1·5000	·7500
12·321	1·1170	·6930
13·245	0·7250	·4900
14·295	0·4330	·3070
14·548	0·3930	·1580
14·836	0·0480	·0930
15·000	0(TE)	0
L_e reading	22 cm	$\alpha_c = 4°$

● – PRESSURE TAPPING

CHORD = 15 CMS.
THICKNESS = 15%
CAMBER = 10%

FIG. 2a – CAMBERED JOUKOWSKY AIRFOIL

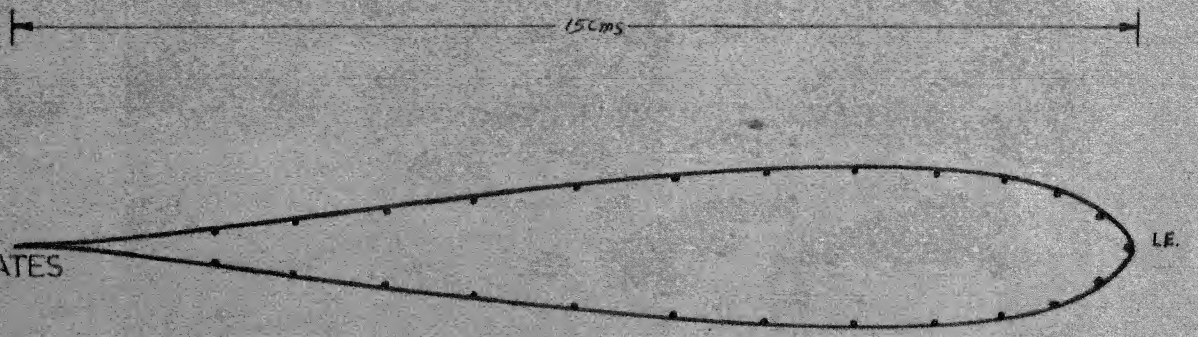

AIRFOIL CO-ORDINATES

X(cms)	Y(cms)
0	0 LE
.114	.298
.452	.575
1.005	.808
1.755	.983
2.679	1.093
3.756	1.125
4.935	1.092
6.198	1.001
7.500	.866
8.902	.705
10.065	.535
11.250	.375
12.321	.237
13.245	.130
14.295	.058
14.548	.018
14.886	.002
15.000	0 TE

LE radius = .253cm

• PRESSURE TAPPINGS

CHORD = 15 CMS.
THICKNESS = 15%

FIG 2b - SYMMETRICAL JOUKOWSKY AIRFOIL

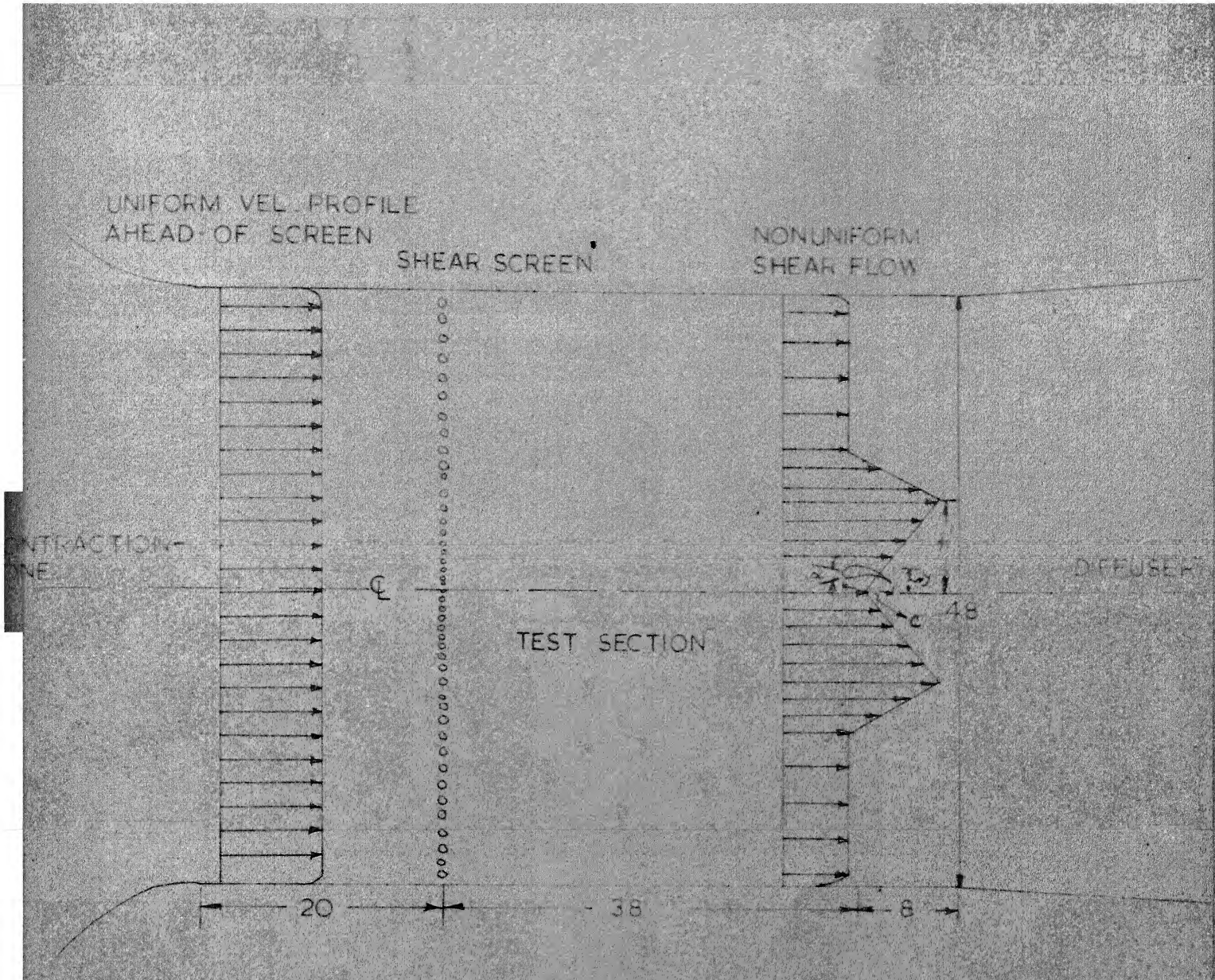

FIG 3 _ SCHEMATIC SKETCH OF THE EXPERIMENTAL SET-UP IN THE 2-D TEST SECTION

SCALE 1/12
ALL DIMENSIONS IN INCHES

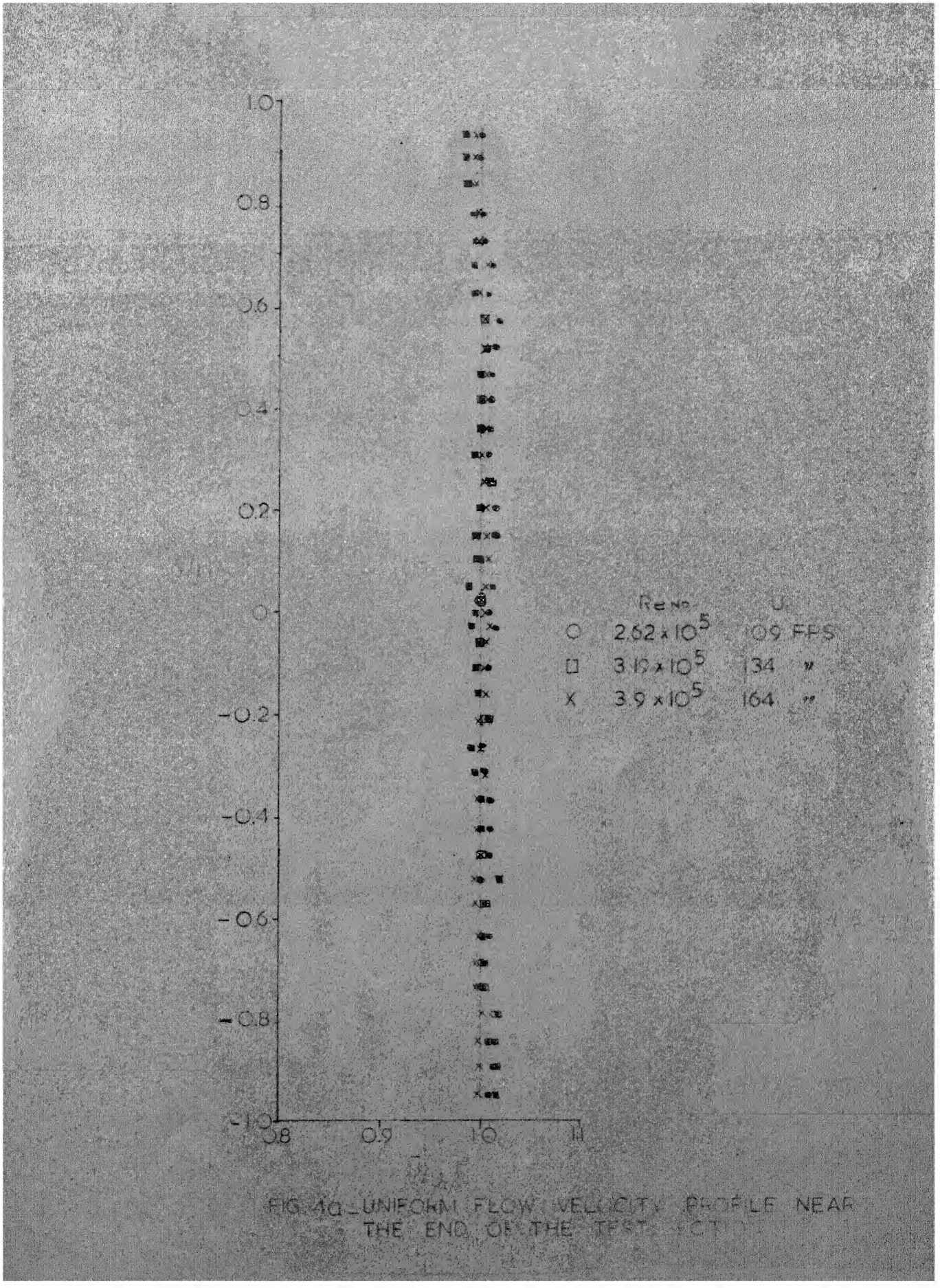

FIG. 40 - UNIFORM FLOW VELOCITY PROFILE NEAR THE END OF THE TEST SECTION

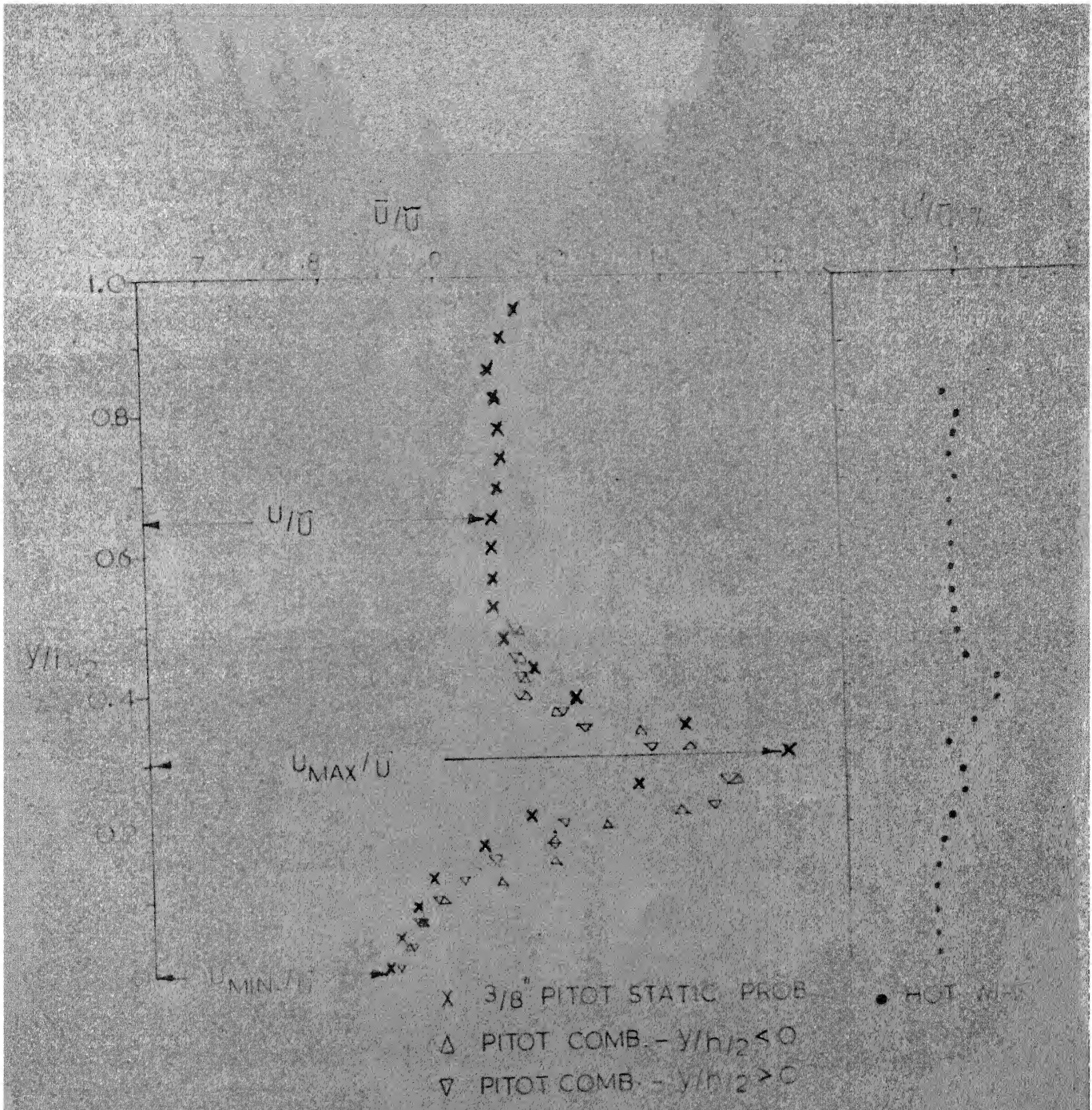

FIG 4b_MEAN VELOCITY PROFILE, I=0.248

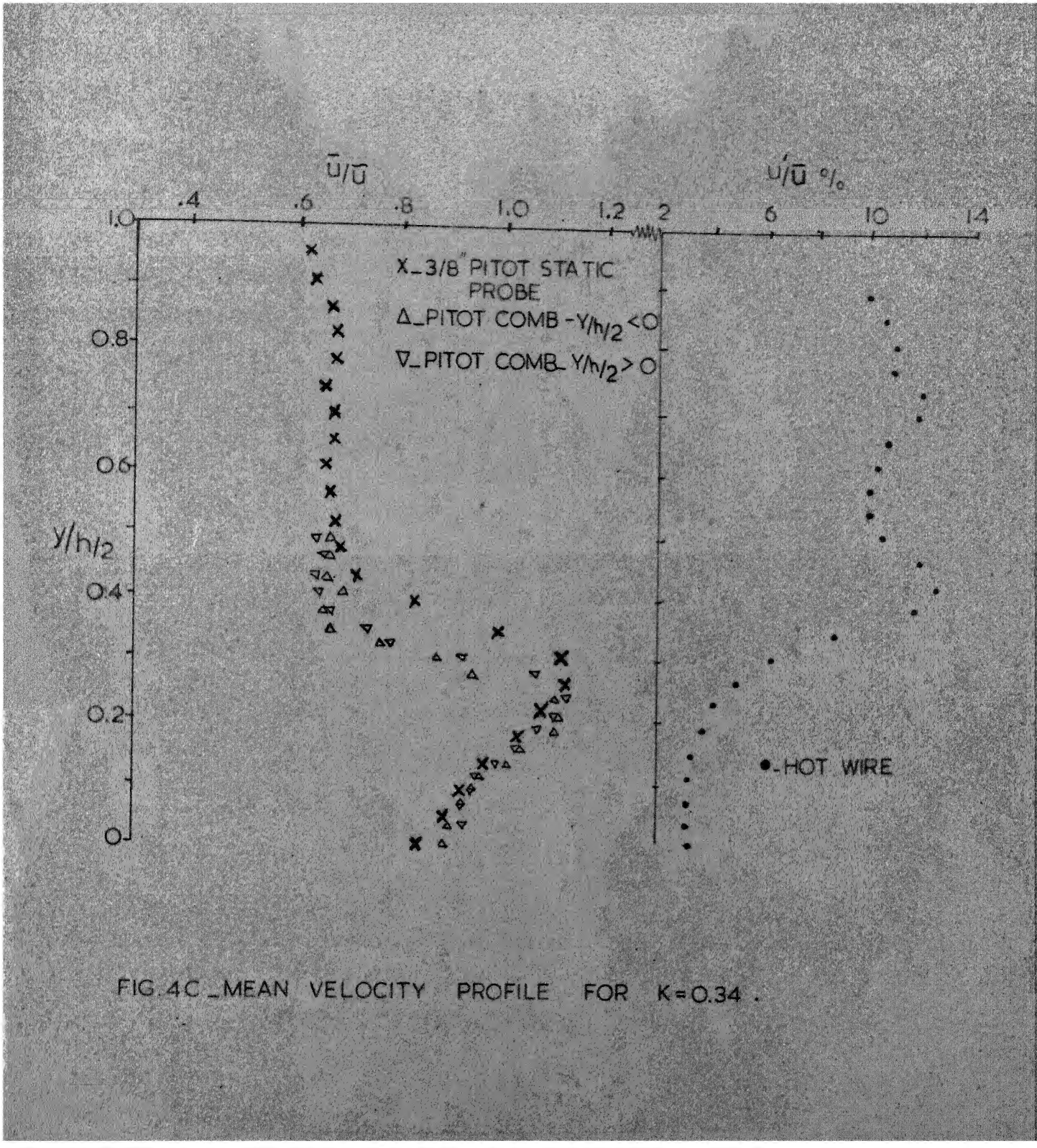

FIG. 4C _MEAN VELOCITY PROFILE FOR K = 0.34 .

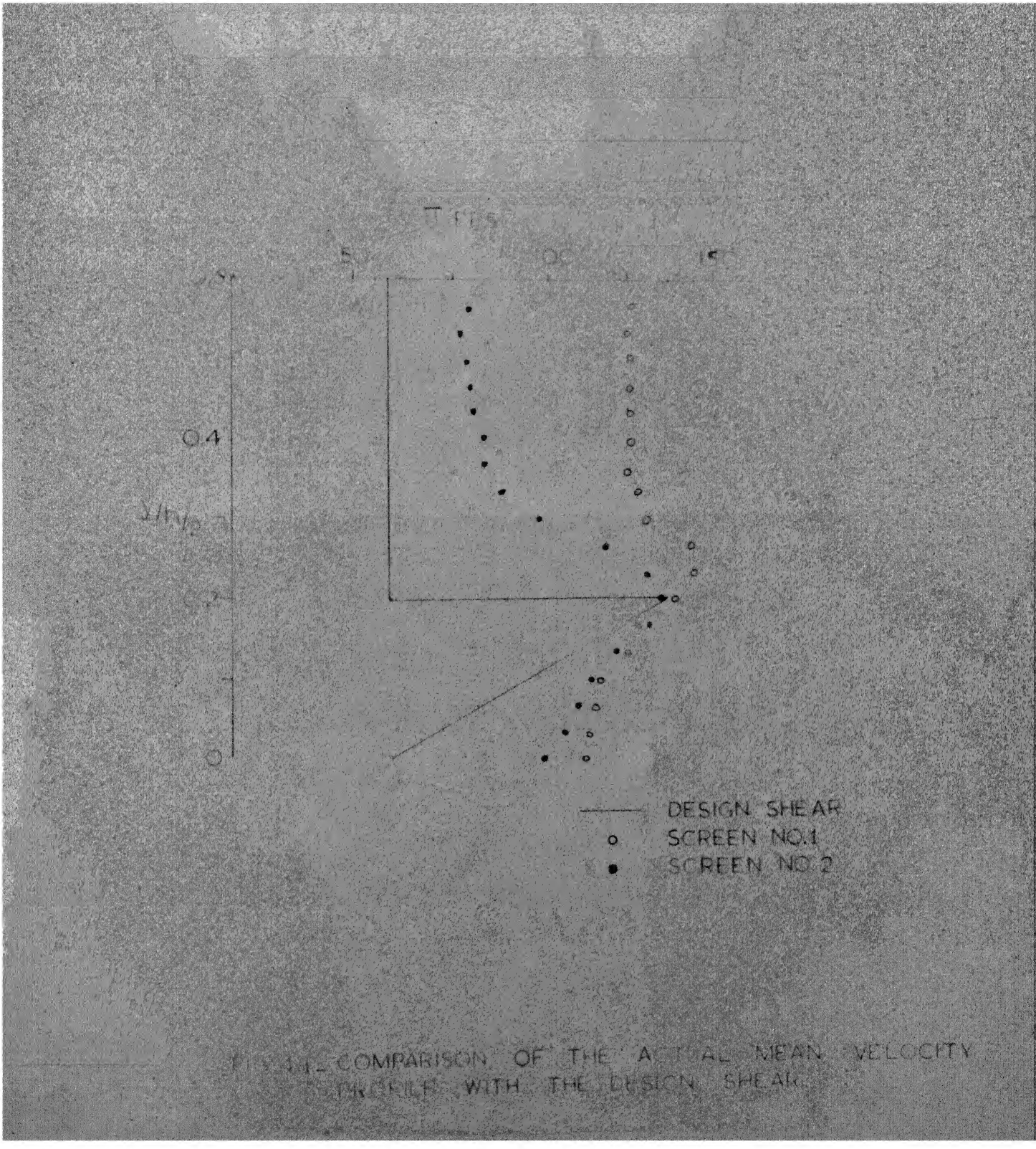

FIG. 11 - COMPARISON OF THE ACTUAL MEAN VELOCITY PROFILE WITH THE DESIGN SHEAR

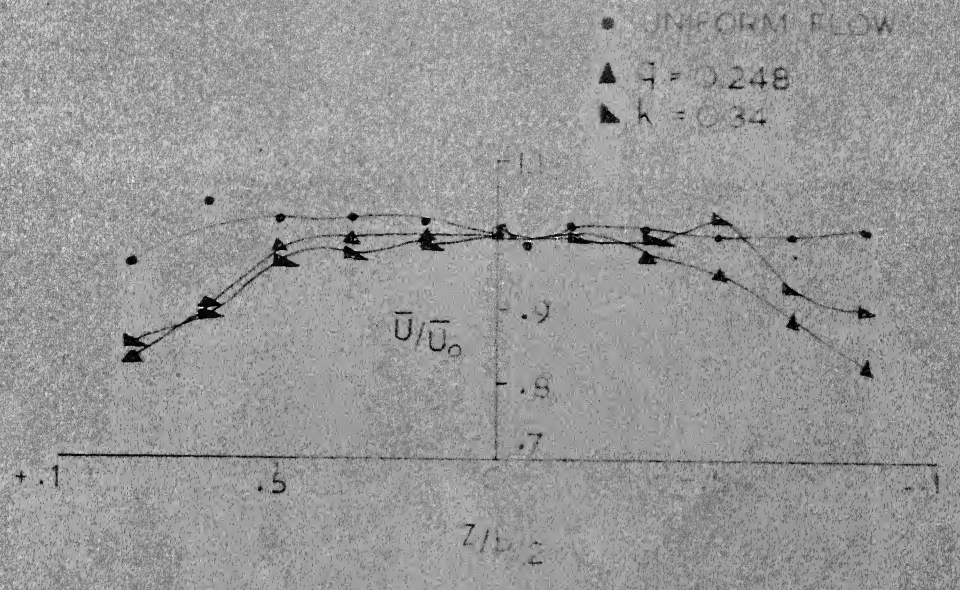

Fig. 4e - SPANWISE VELOCITY PROFILE AT THE TUNNEL CENTRE LINE, $y/D/2=0$

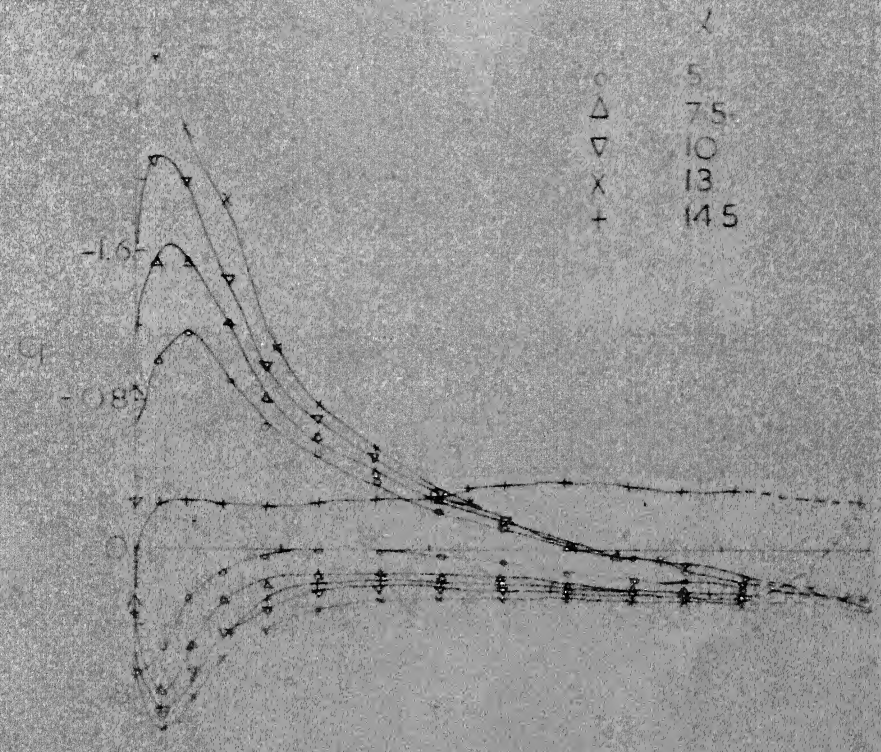

FIG. 5 PRESSURE DISTRIBUTION OVER SYMMETRICAL JOUKOWSKY AIRFOIL IN UNIFORM FLOW

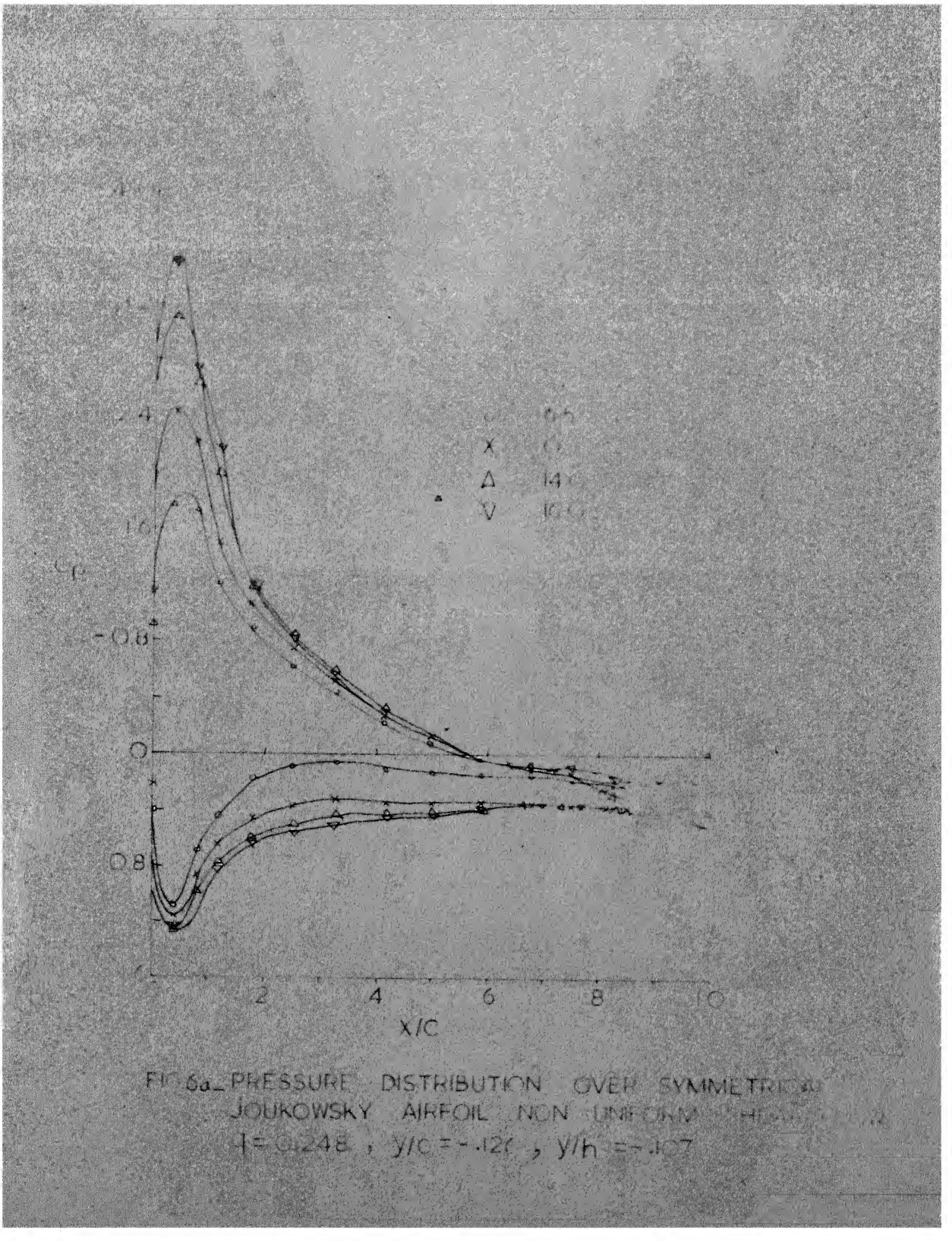

FIG 6a_PRESSURE DISTRIBUTION OVER SYMMETRICAL JOUKOWSKY AIRFOIL NON UNIFORM
$\tau = 0.248$, $y/c = -.12$, $y/h = -.107$

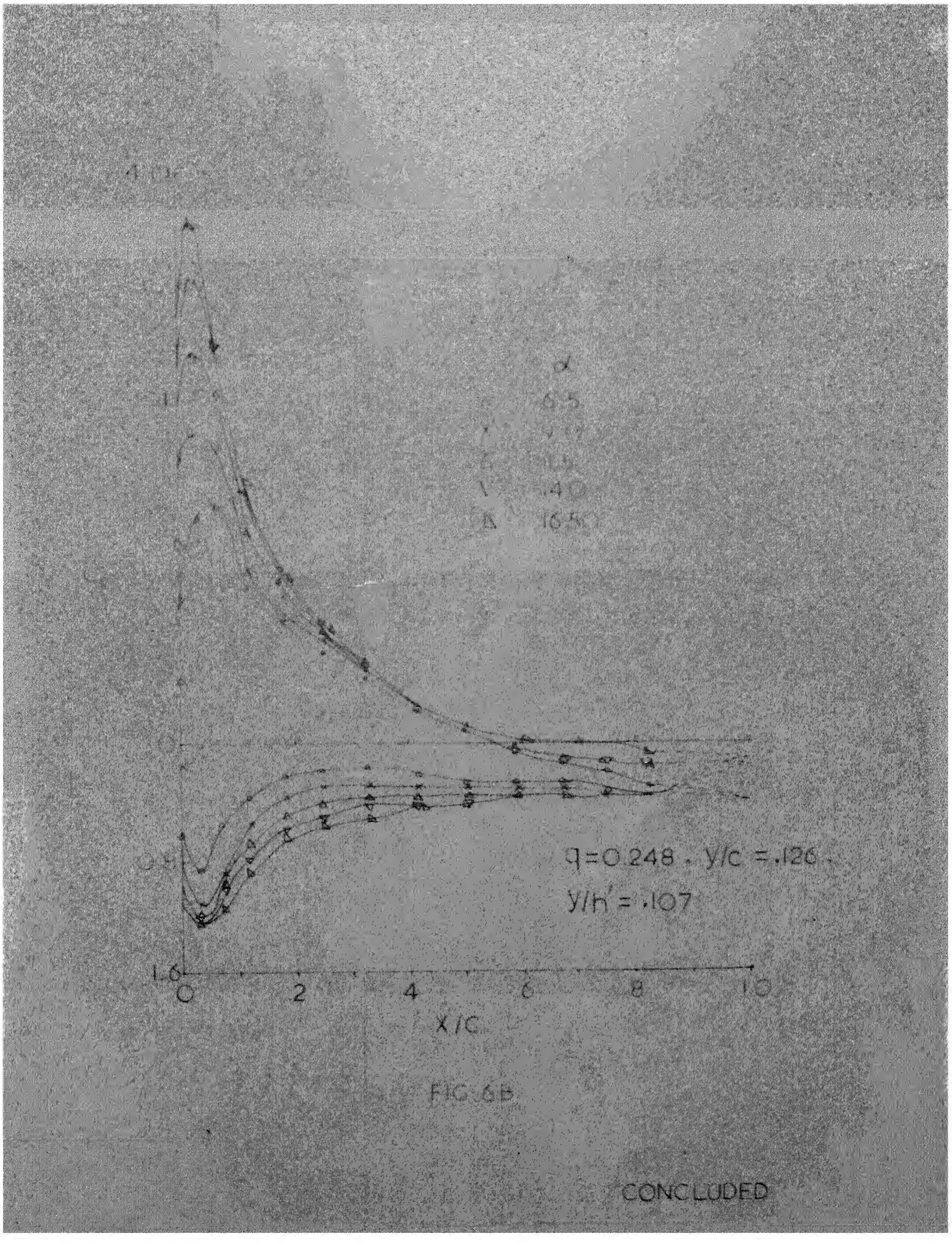

FIG. 6B

CONCLUDED

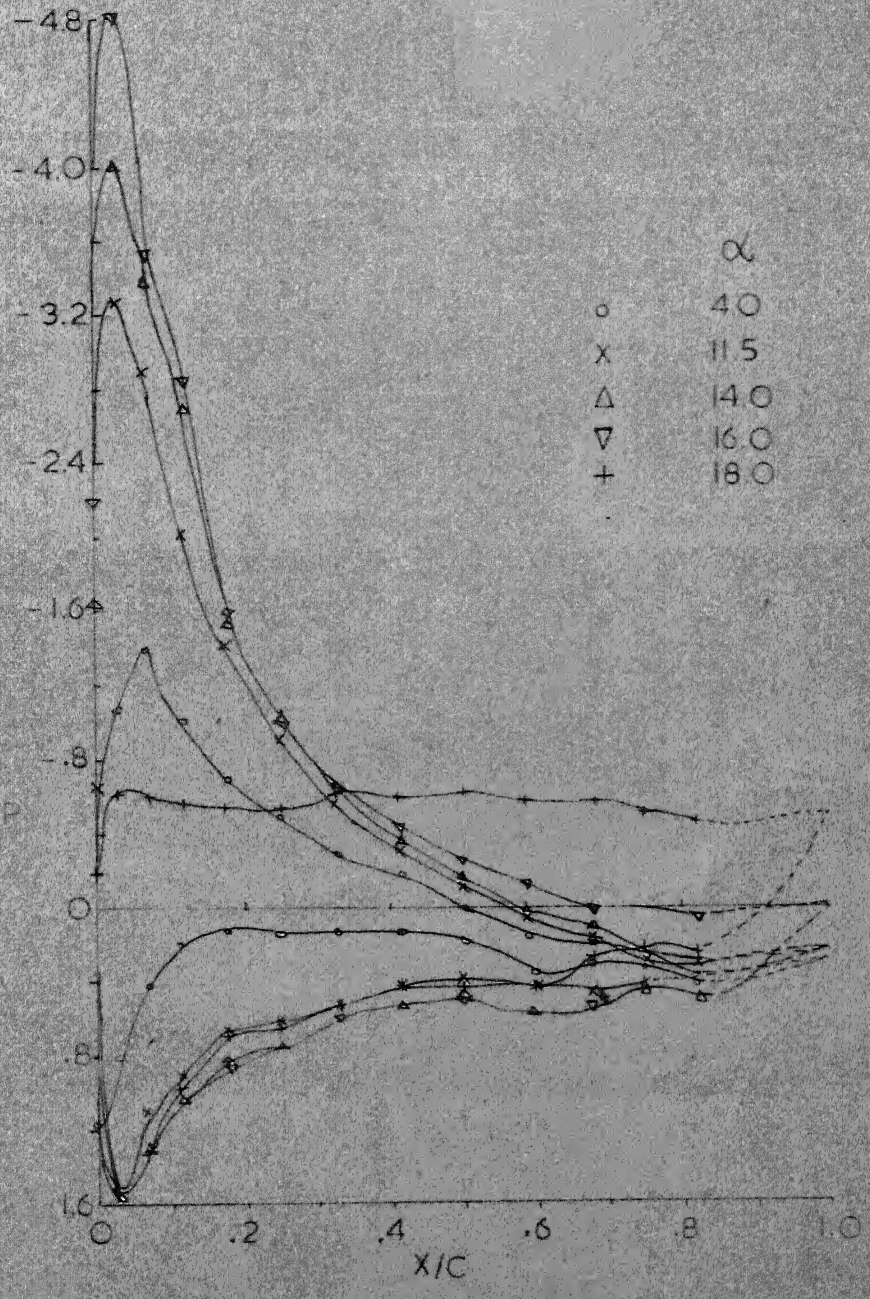

FIG 7a - PRESSURE DISTRIBUTION OVER SYMMETRICAL JOUKOWSKY AIRFOIL IN NON UNIFORM SHEAR FLOW
$k = 0.34$; $y/c = -.126$; $y/h' = -.11$

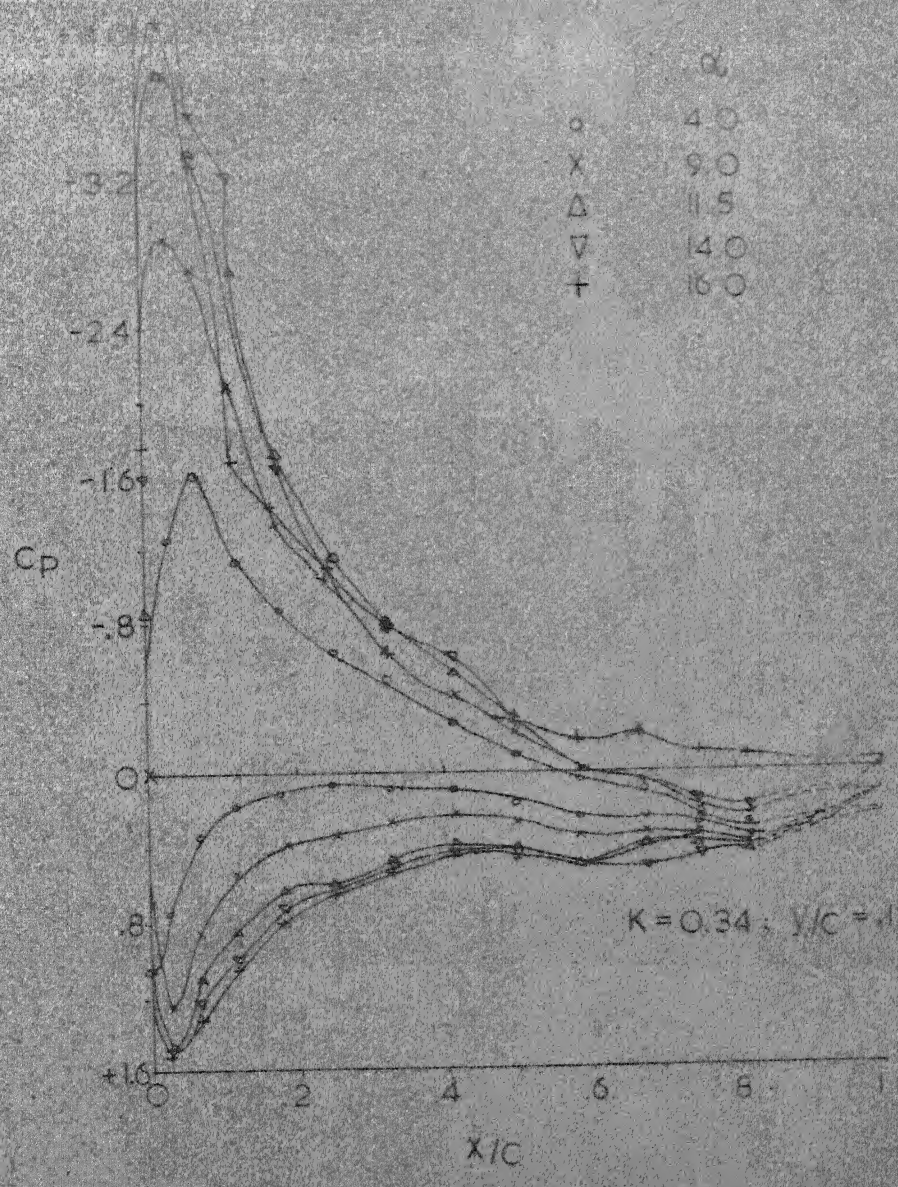

FIG. 7b

CONCLUDED

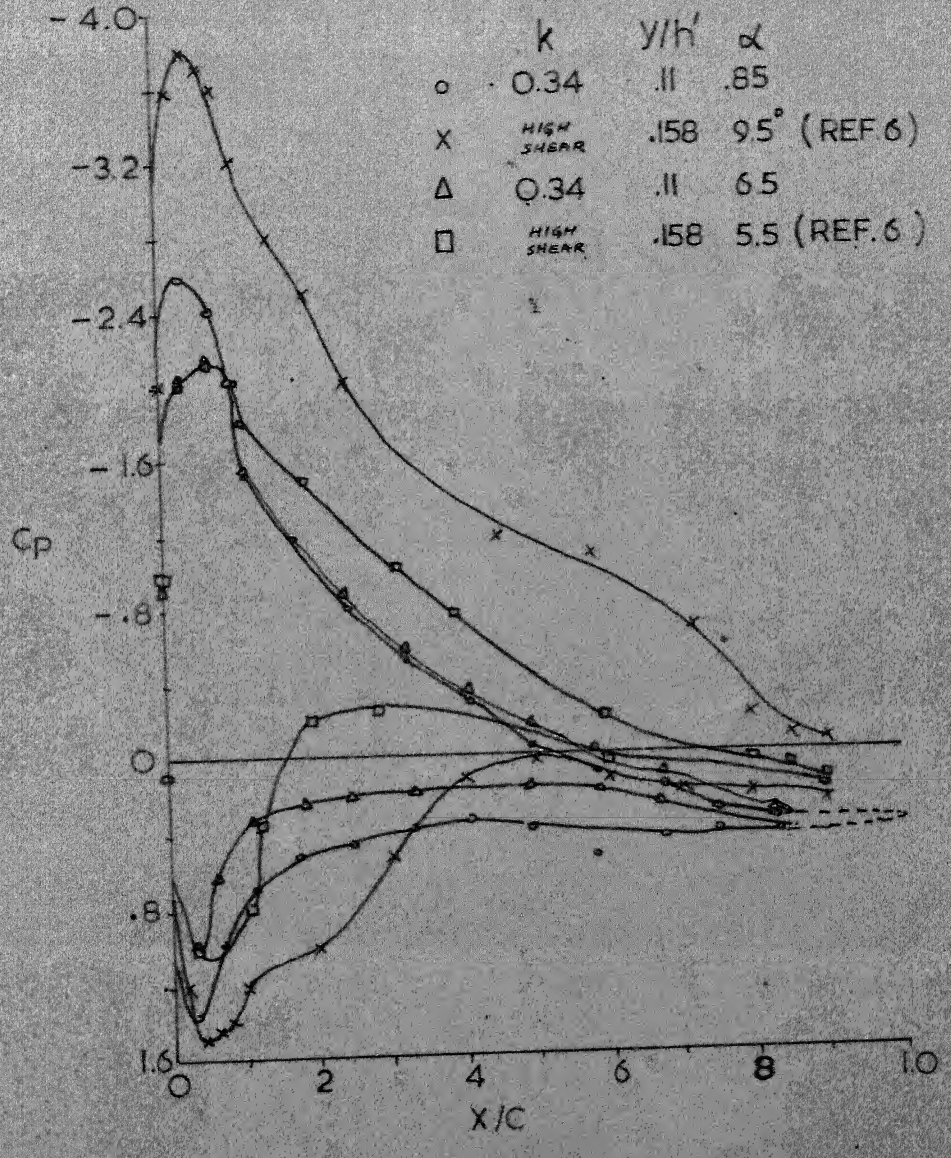

FIG. 7C_COMPARISON OF THE PRESSURE PLOT OF SYMMETRICAL AIRFOIL WITH THAT OF REF. 6

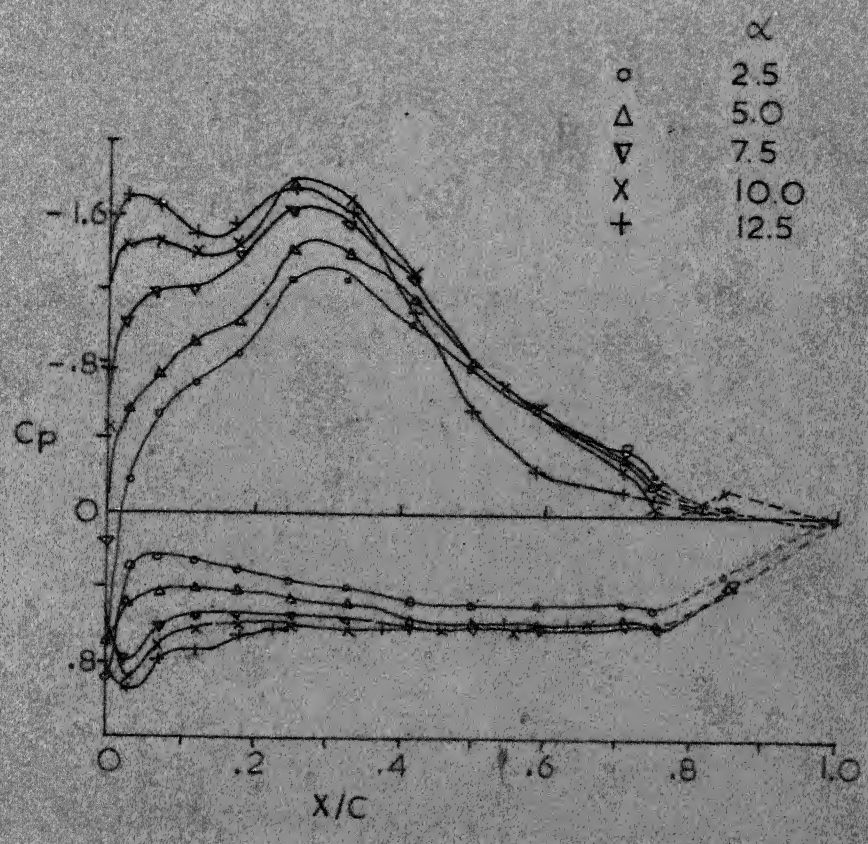

FIG. 8_ PRESSURE DISTRIBUTION OVER CAMBERED JOUKOWSKY AIRFOIL IN UNIFORM FLOW.

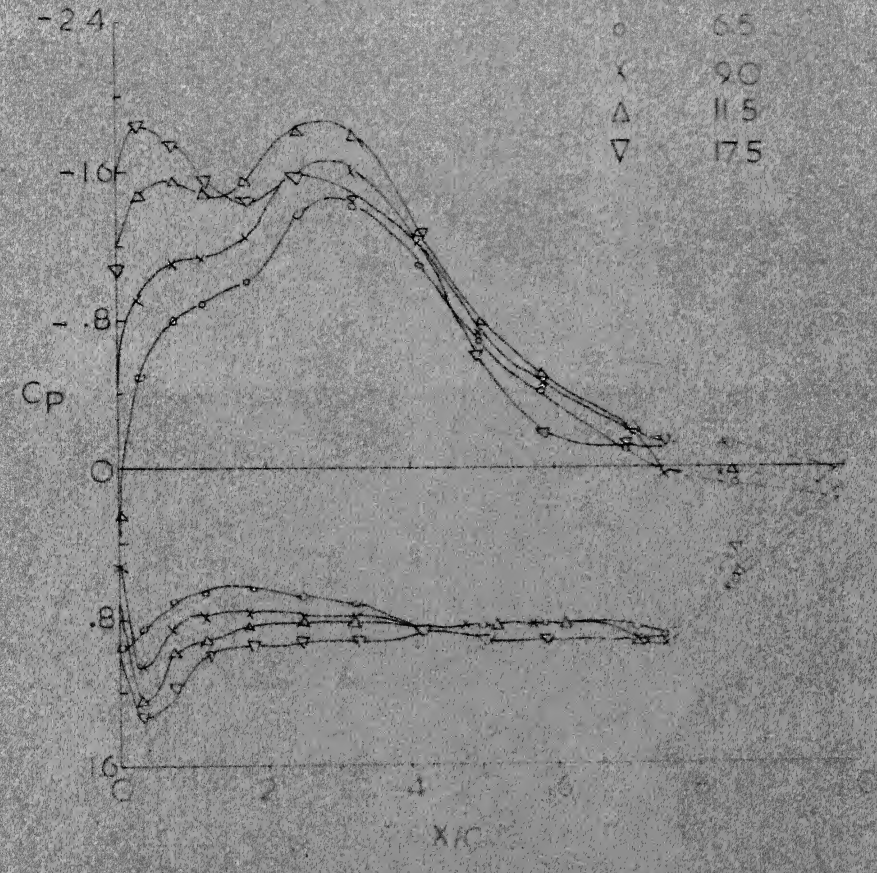

FIG 9a_PRESSURE DISTRIBUTION OVER A CIRCULAR JOUKOWSKY AIRFOIL IN NON UNIFORM SHEAR FLOW. q = 0.248, y/c = -.126, y/h = -.107

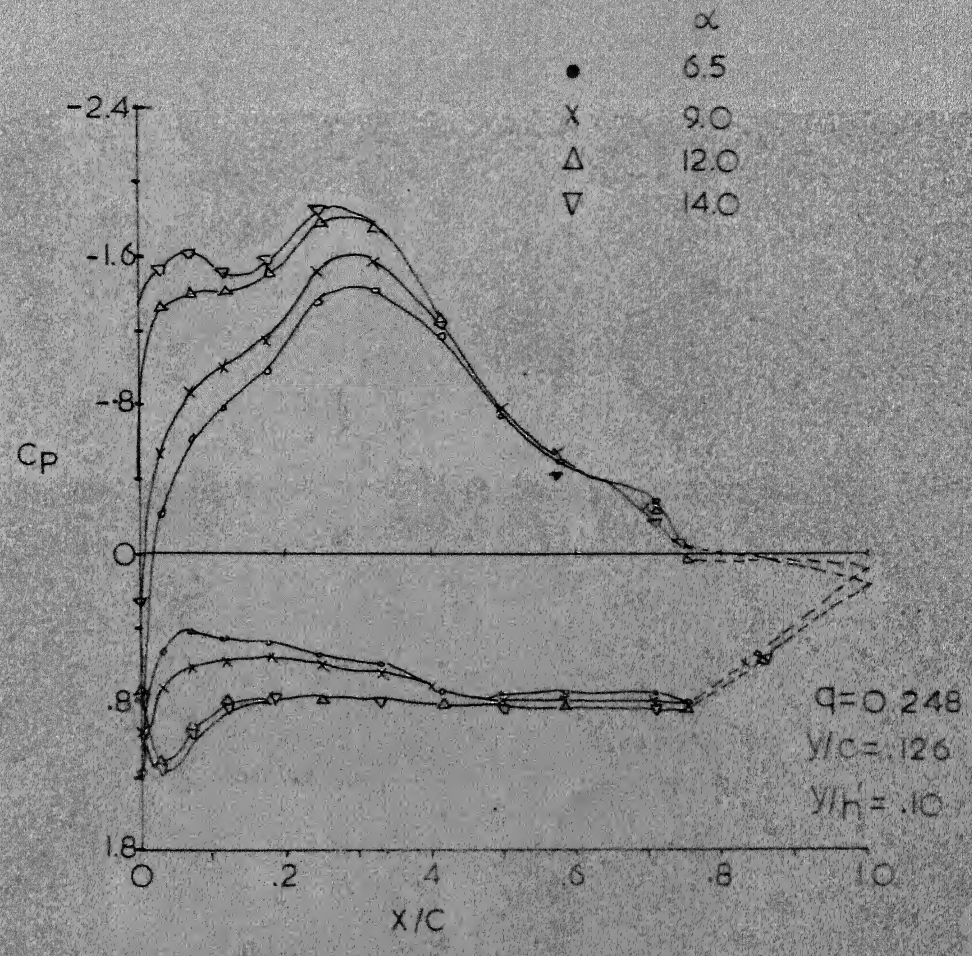

FIG. 9b

CONCLUDED

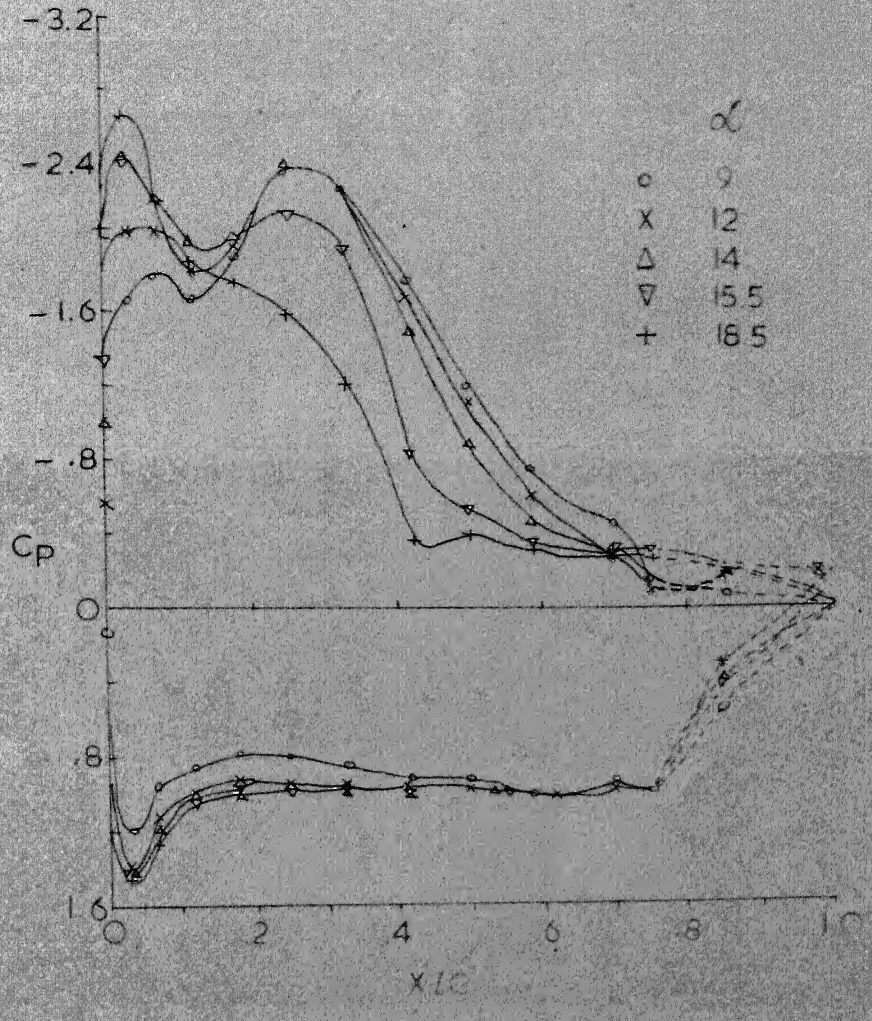

FIG. [illegible] PRESSURE DISTRIBUTION [illegible] AIRFOIL
JOUKOWSKY AIRFOIL [illegible]
X = [illegible] Y/C = [illegible]

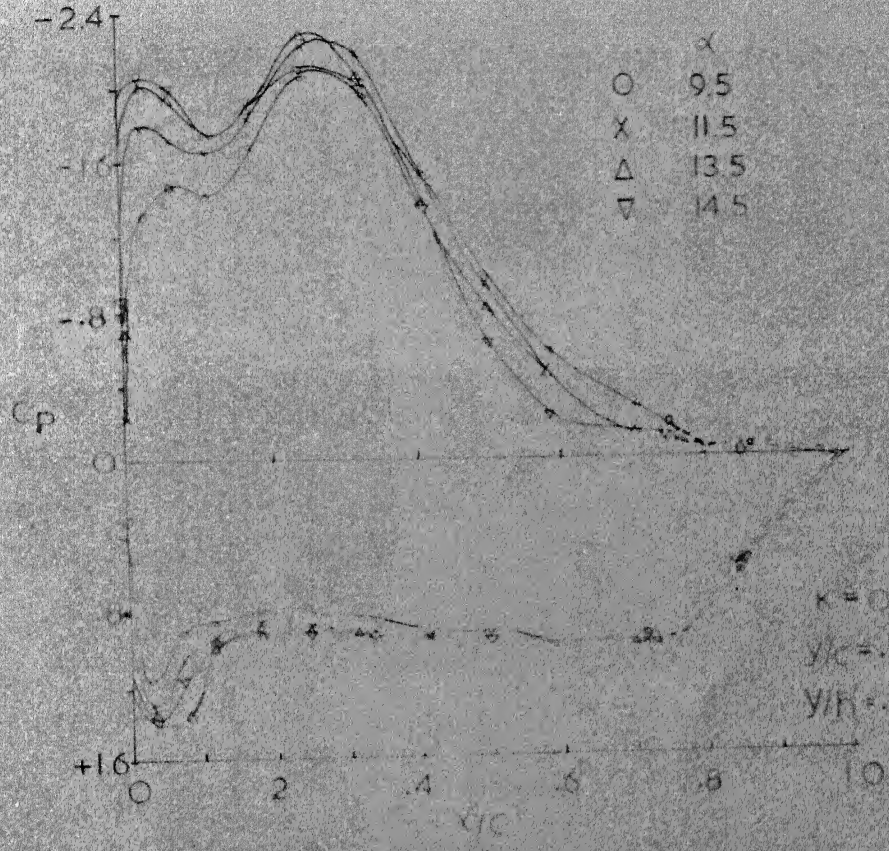

FIG. 10b

CONCLUDED

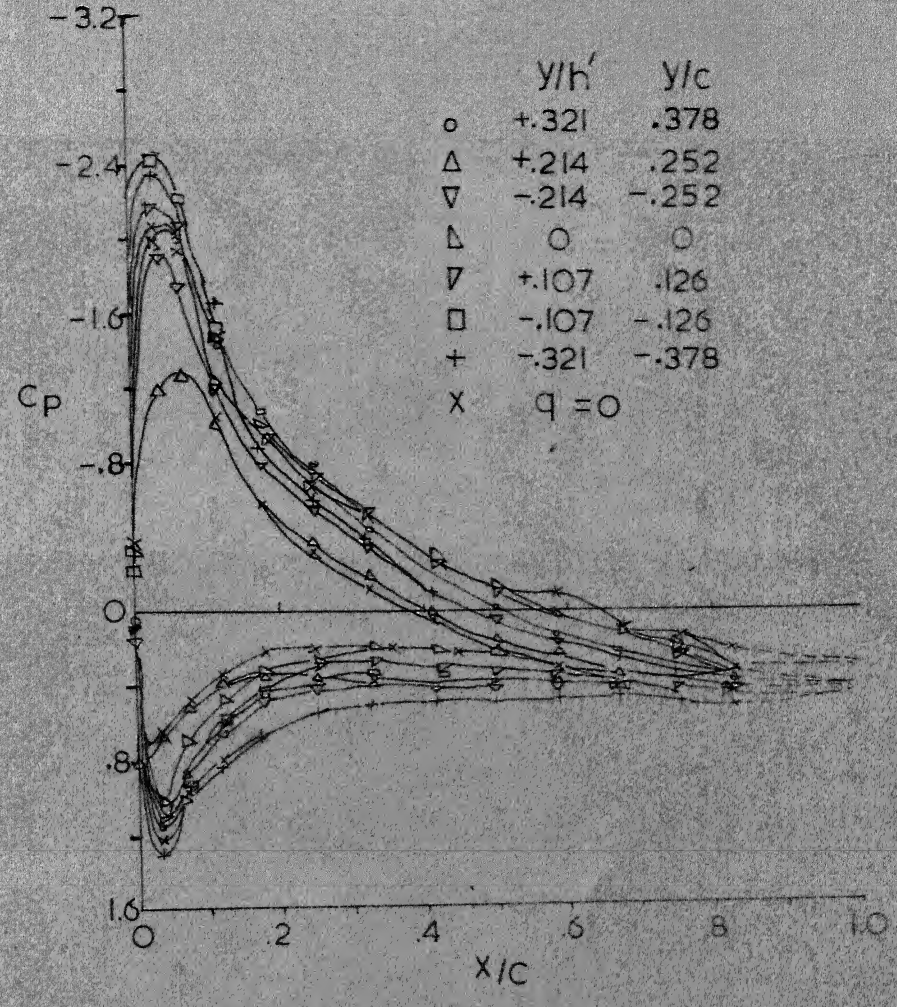

FIG. IIa_EFFECT OF VERTICAL LOCATION ON PRESSURE DISTRIBUTION OVER SYMMETRICAL AIRFOIL IN NONUNIFORM SHEAR FLOW
$q = 0.248$; $\alpha = 9°$

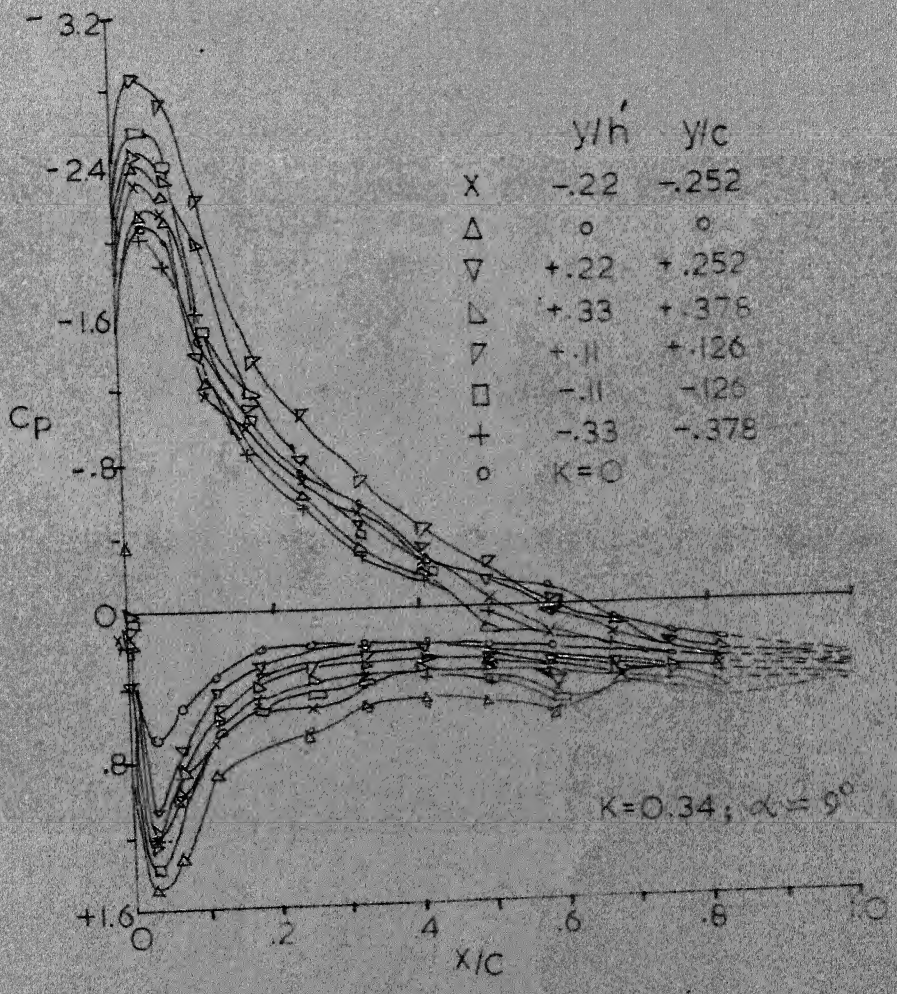

FIG. 11b

CONCLUDED

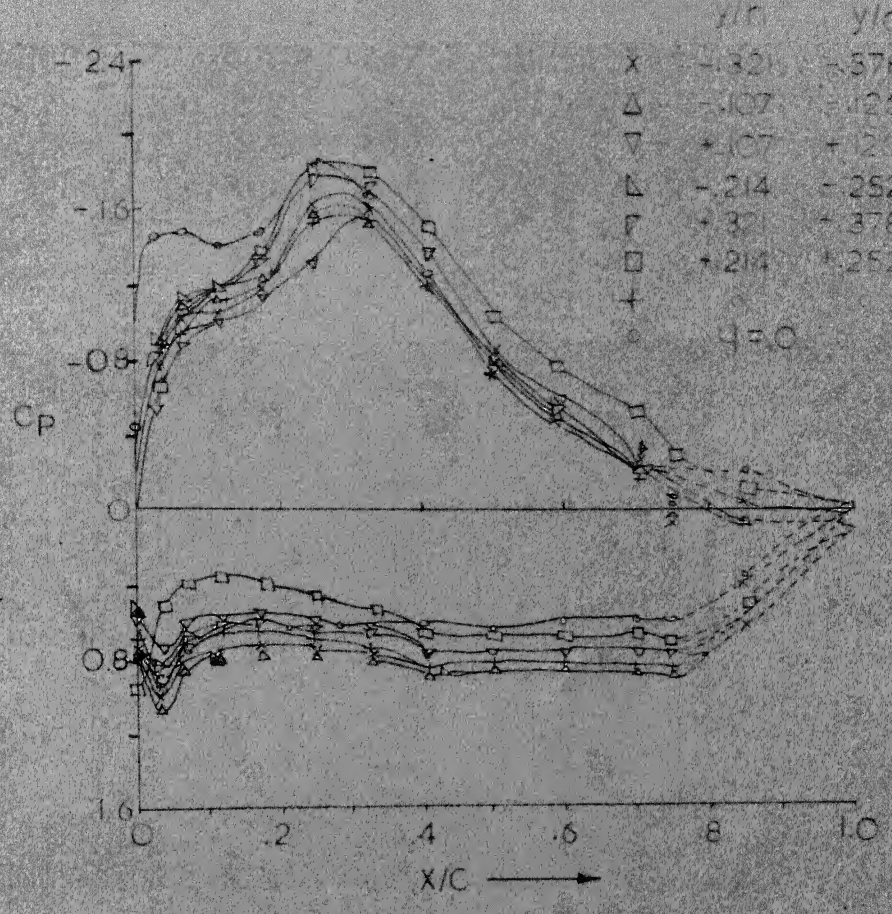

FIG.12a_EFFECT OF VERTICAL LOCATION ON THE PRESSURE DISTRIBUTION OVER THE CAMBERED AIRFOIL IN NON UNIFORM SHEAR FLOW.
$q = 0.248$, $\alpha = 9°$

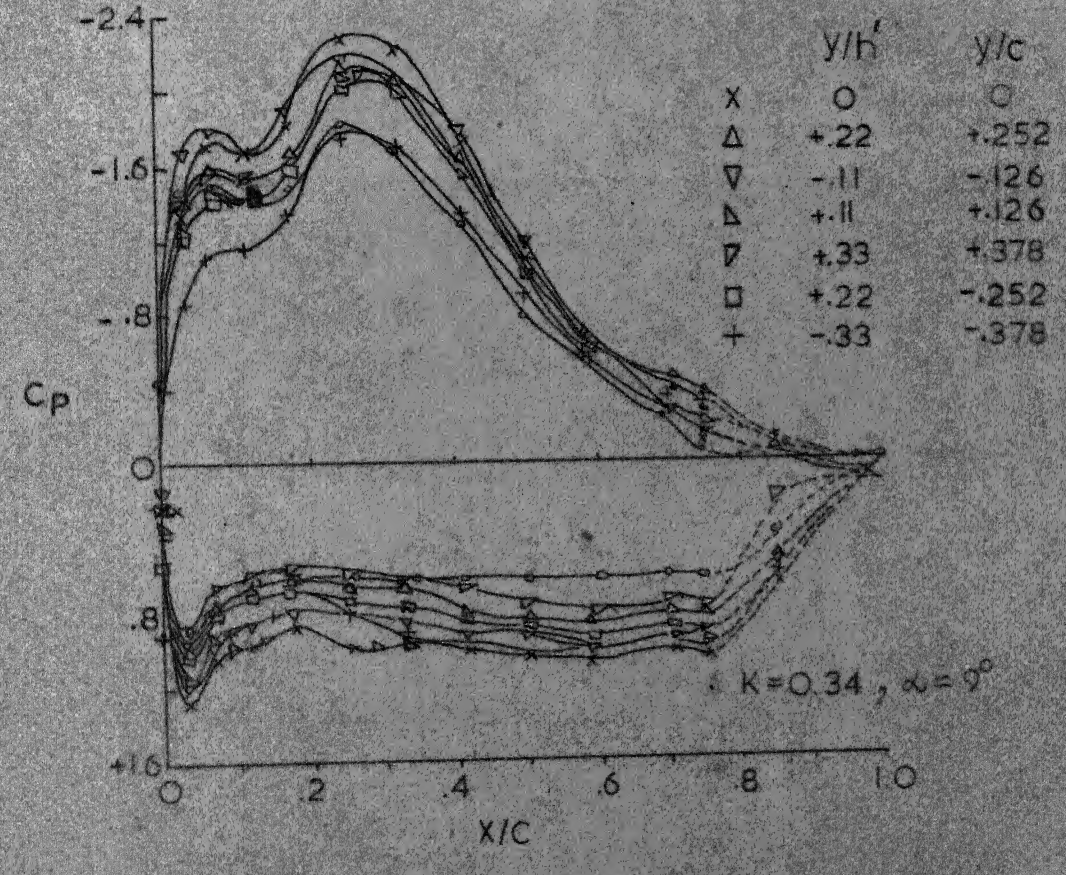

FIG. 12b

CONCLUDED

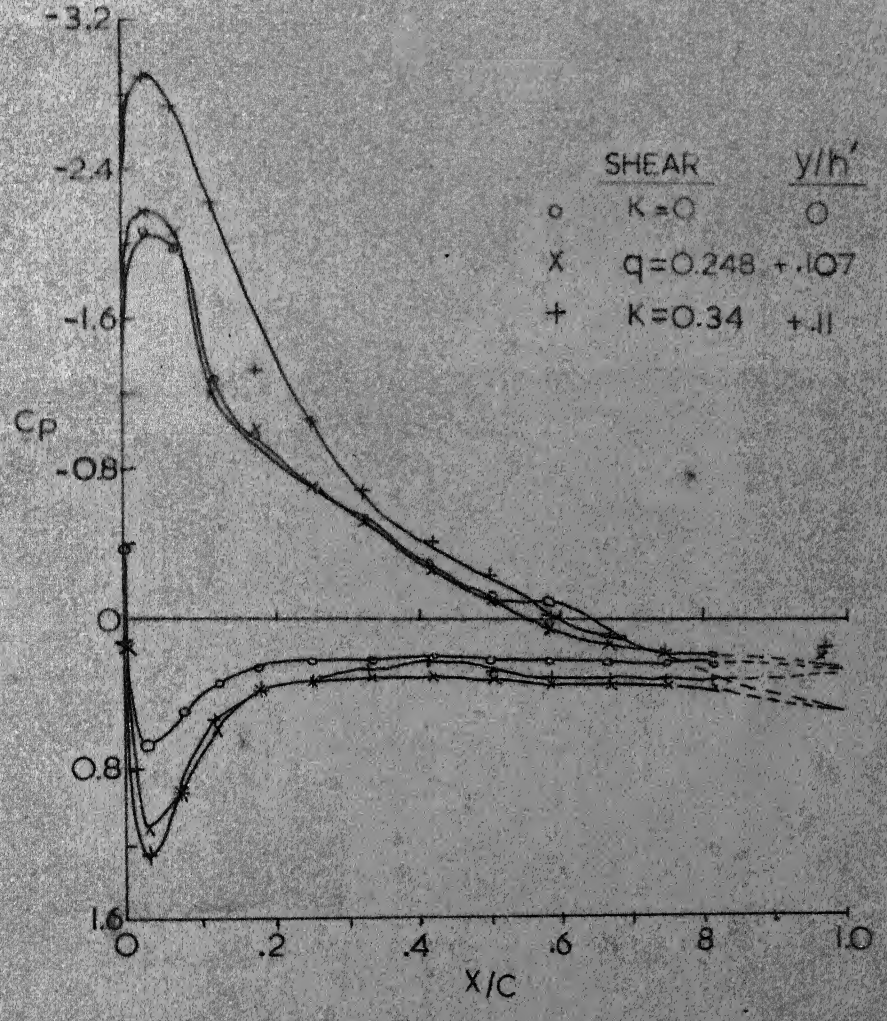

FIG. 13a - EFFECT OF CHANGE IN NON UNIFORM SHEAR OVER PRESSURE DISTRIBUTION OVER SYMMETRICAL AIRFOIL FOR Y/C = .126, $\alpha = 9°$.

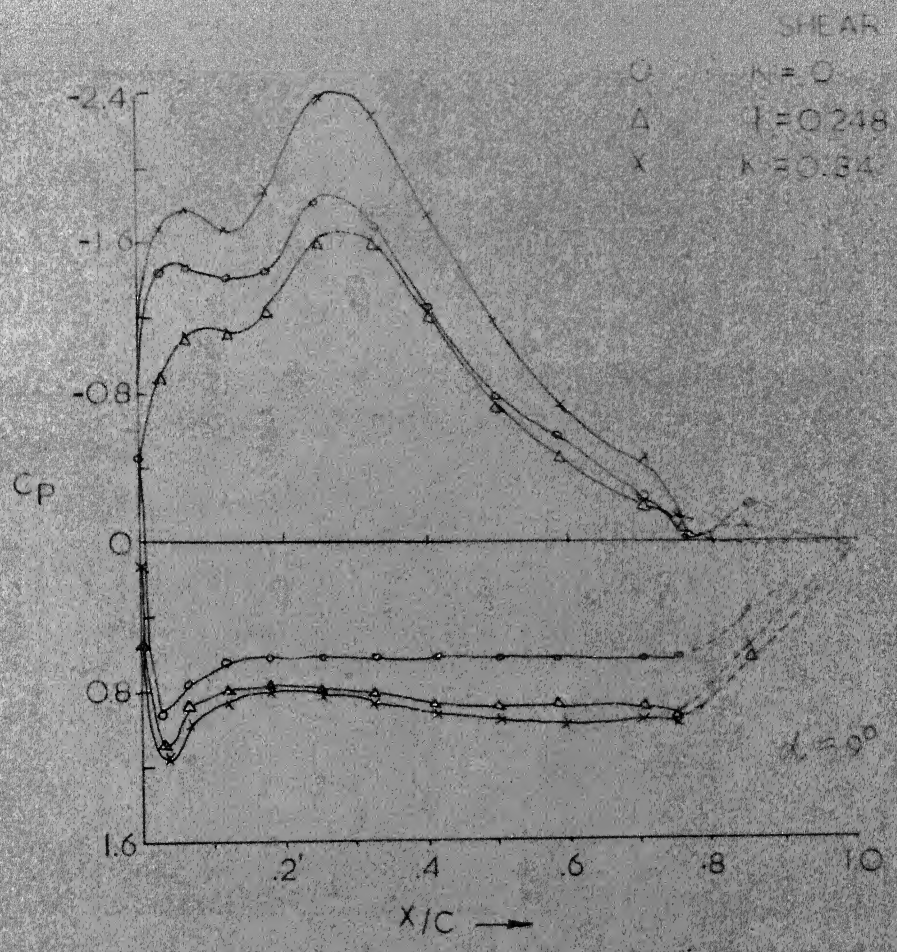

FIG. 13b_CAMBERED AIRFOIL IN NONUNIFORM SHEARFLOW FOR y/C = − 126 , $\alpha \approx 9°$

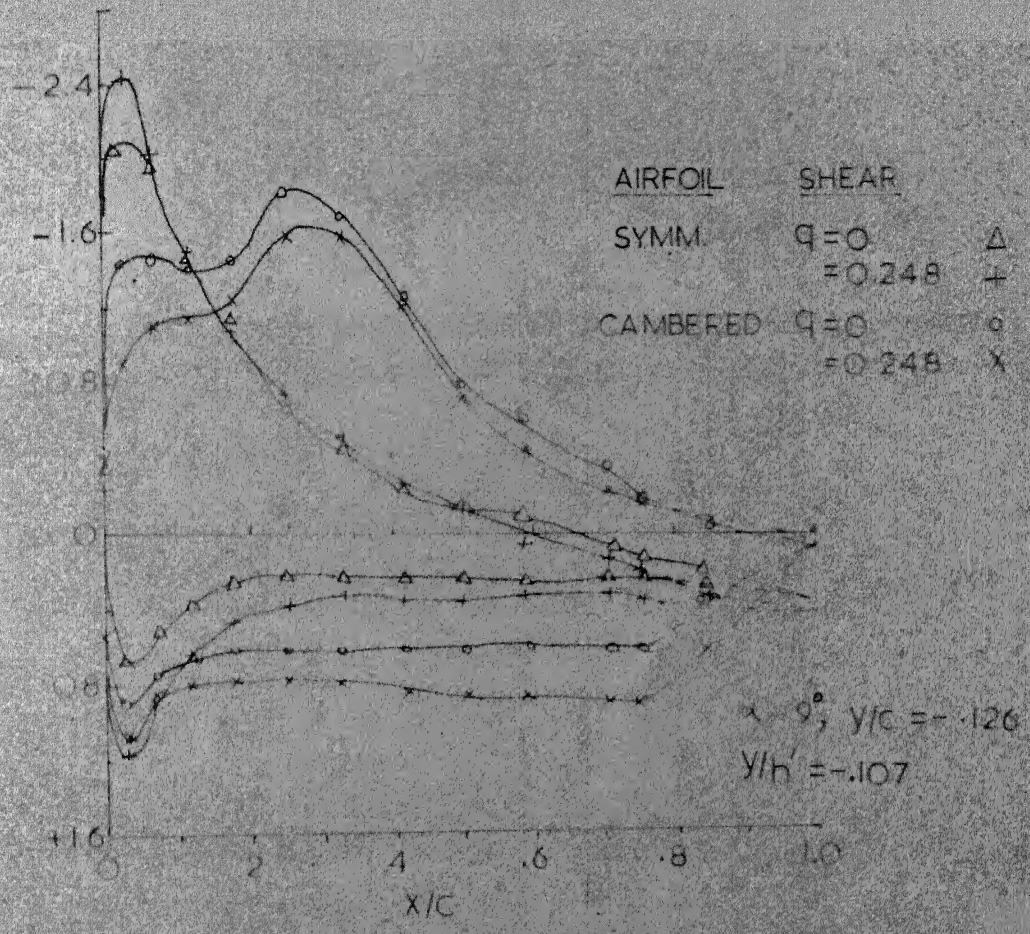

FIG. 14 (1) EFFECT OF CAMBER ON PRESSURE DISTRIBUTION OVER THE AIR FOIL IN NON UNIFORM FLOW.

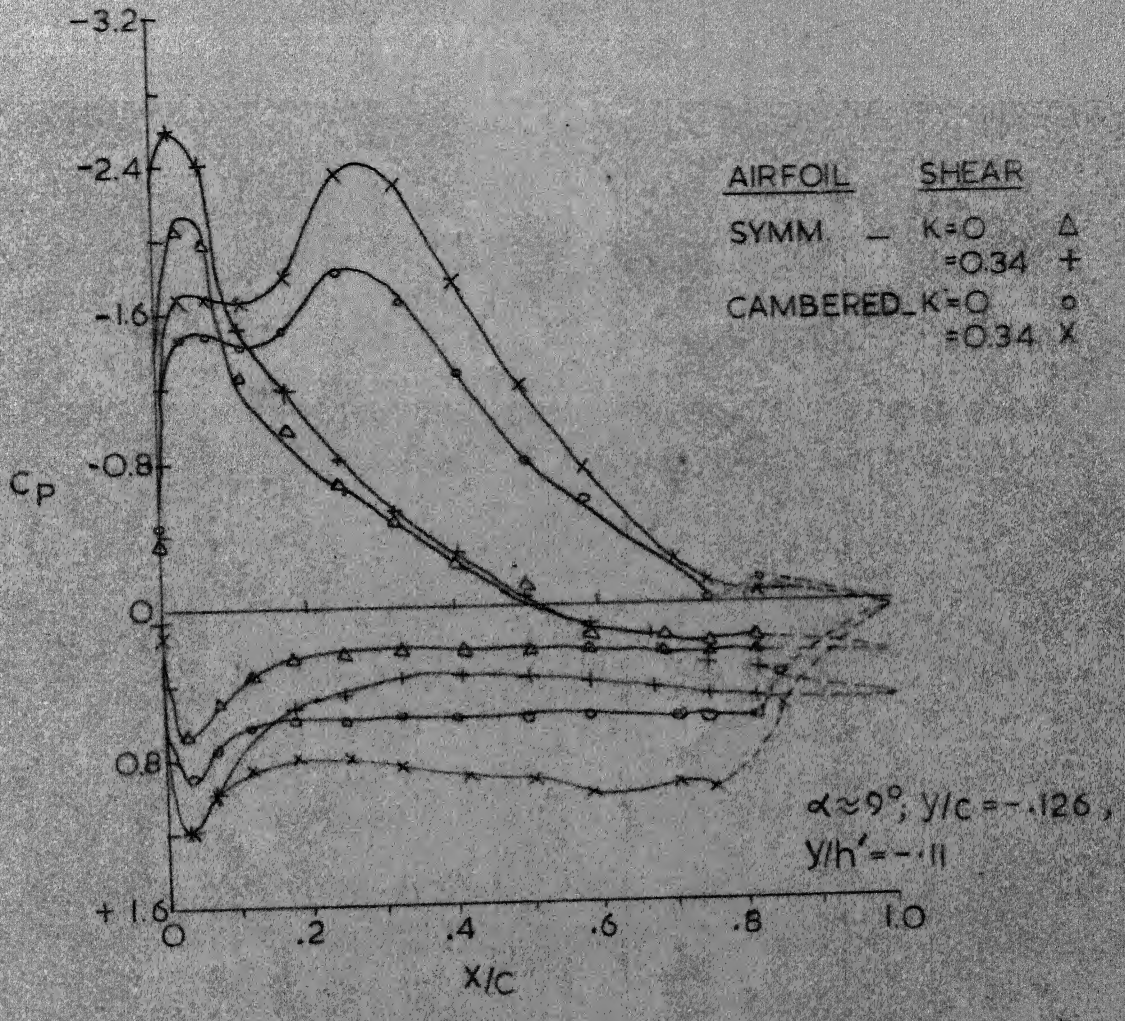

FIG. 14 b.

CONCLUDED

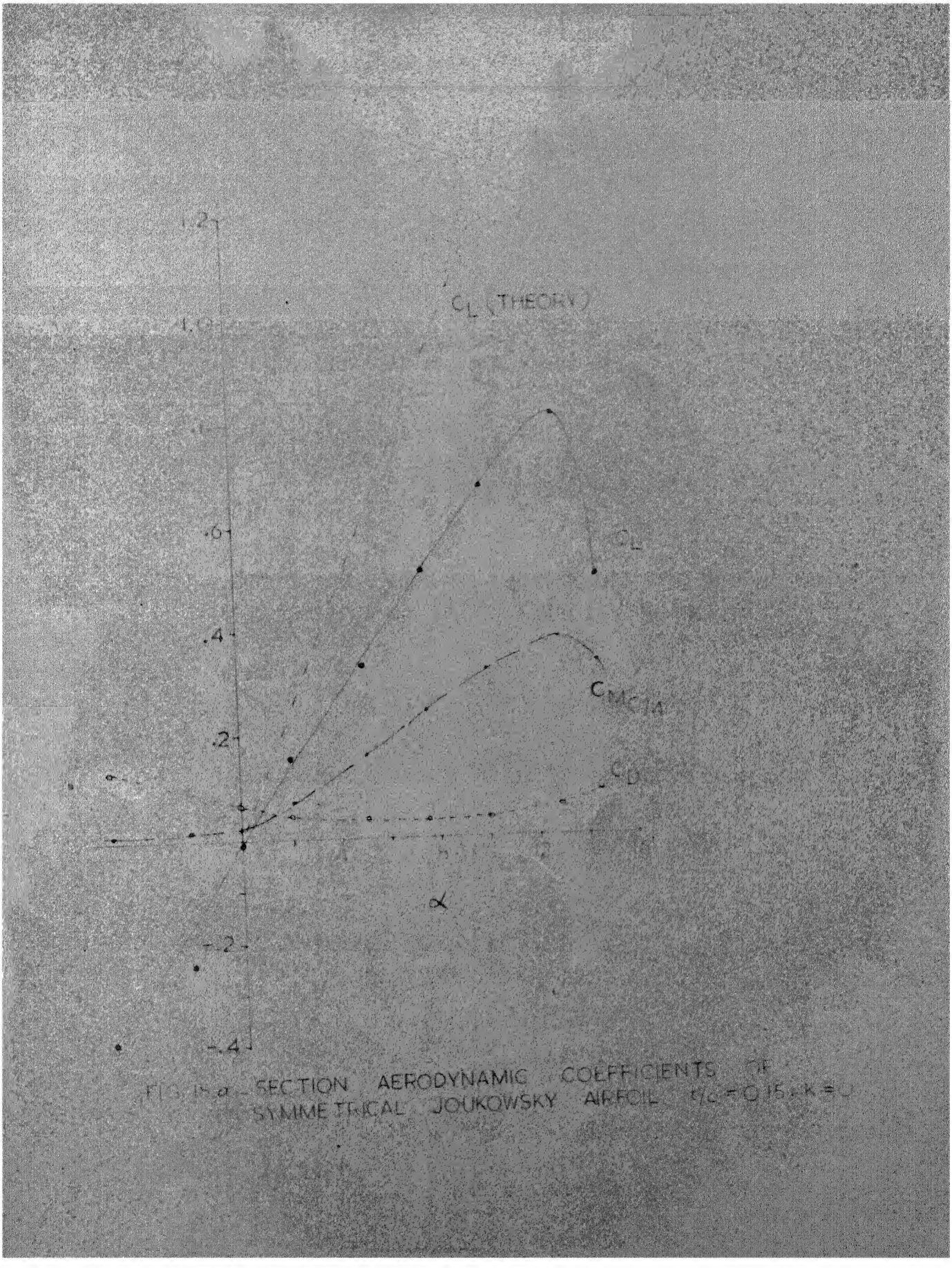

FIG. 14a - SECTION AERODYNAMIC COEFFICIENTS OF SYMMETRICAL JOUKOWSKY AIRFOIL t/c = 0.15, k = 0

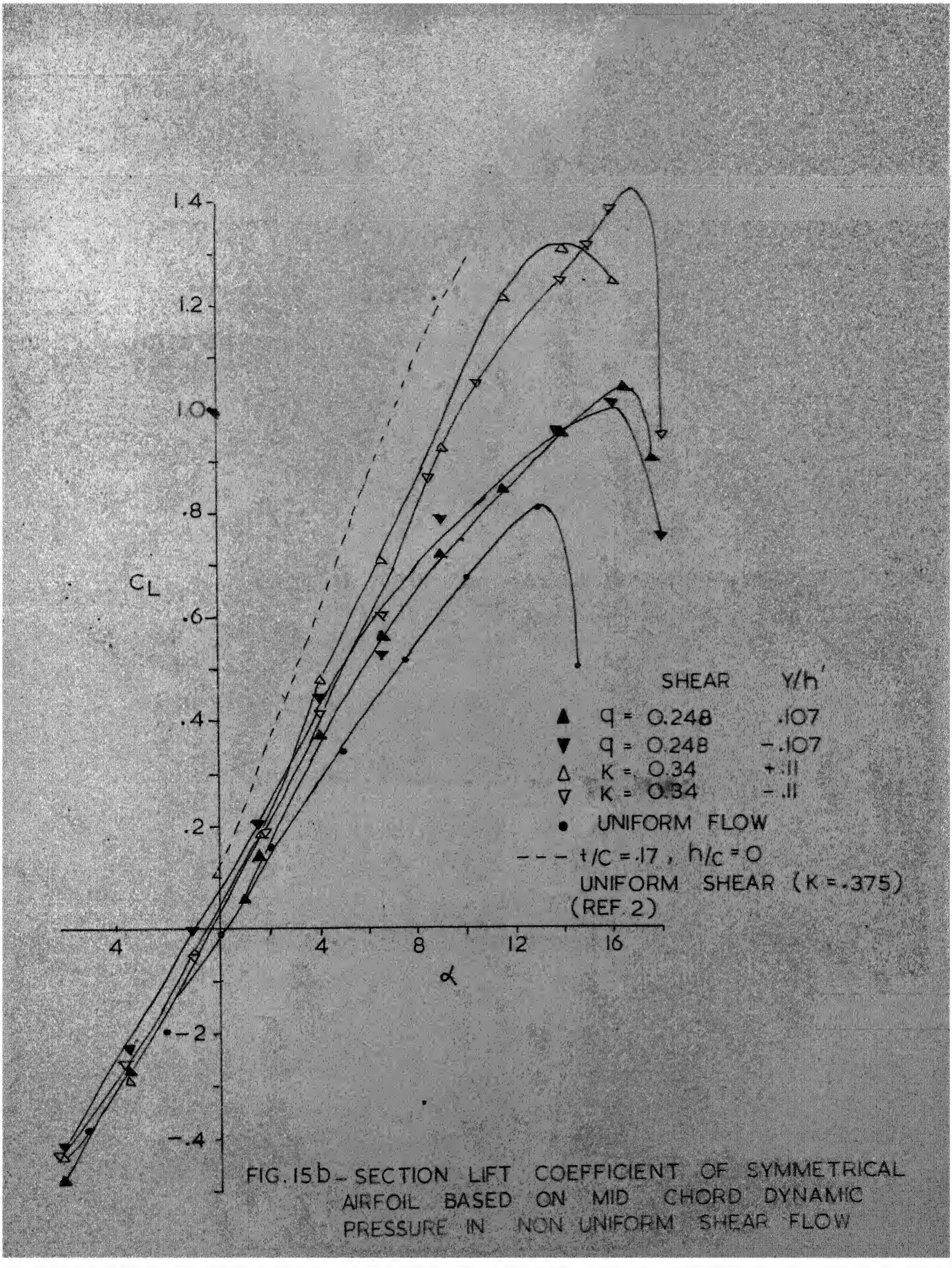

FIG. 15b - SECTION LIFT COEFFICIENT OF SYMMETRICAL AIRFOIL BASED ON MID CHORD DYNAMIC PRESSURE IN NON UNIFORM SHEAR FLOW

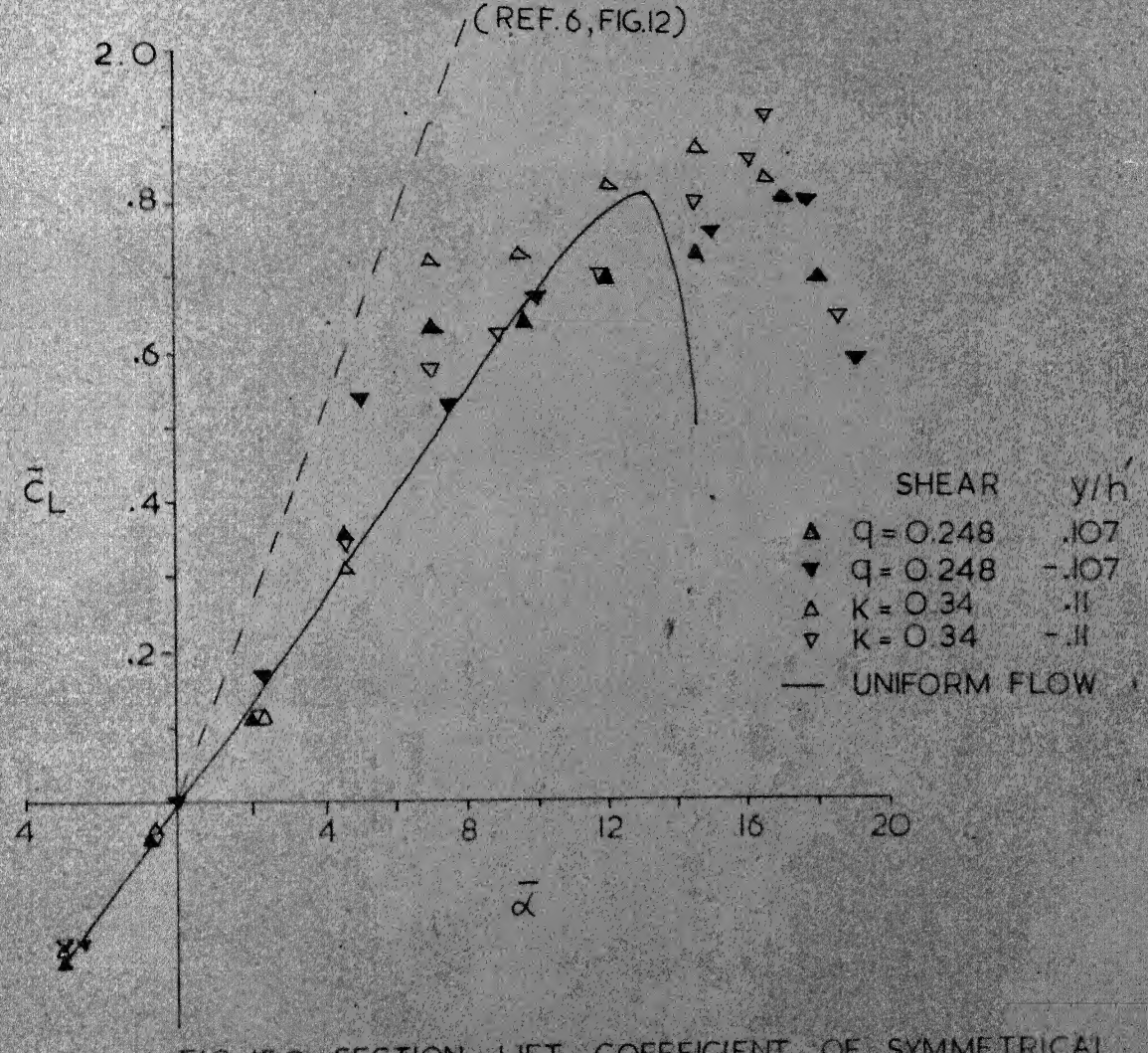

FIG. 15C - SECTION LIFT COEFFICIENT OF SYMMETRICAL AIRFOIL BASED ON STAGNATION STREAM LINE DYNAMIC PRESSURE, NON UNIFORMLY SHEARED FLOW.

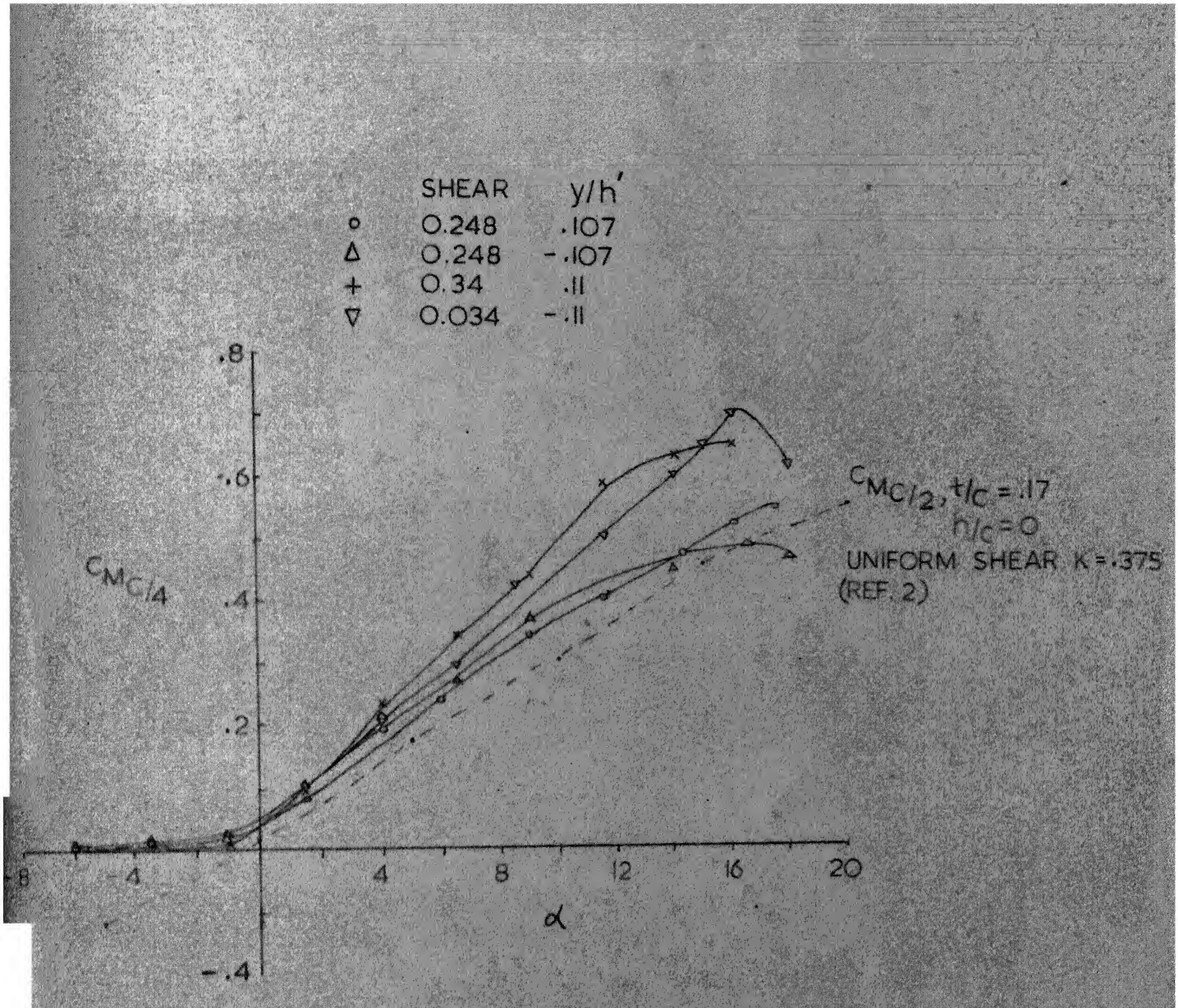

FIG 15d – SECTION PITCHING MOMENT COEFFICIENTS FOR SYMM. AIRFOIL IN NON UNIFORM SHEAR FLOW

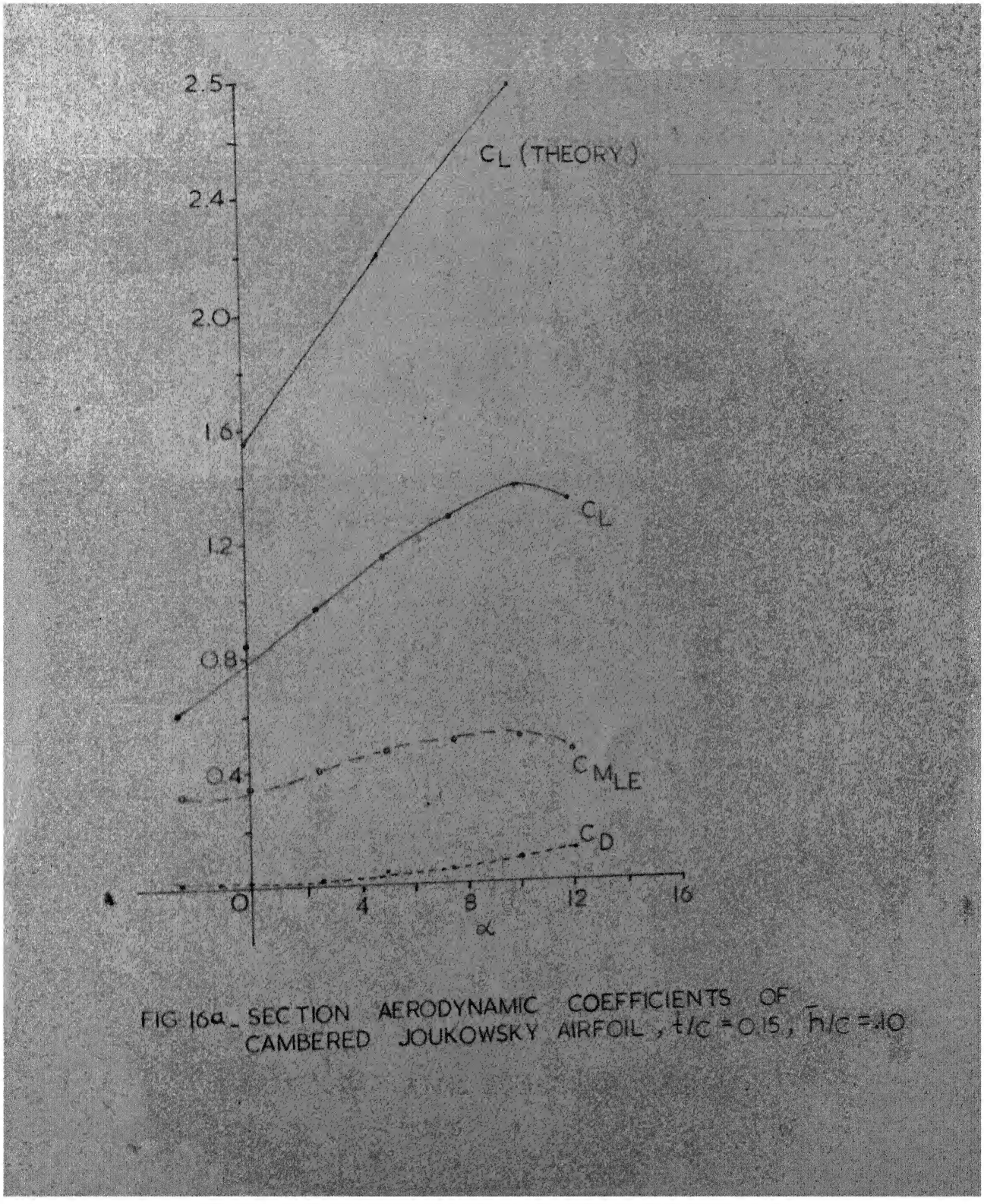

FIG 16a - SECTION AERODYNAMIC COEFFICIENTS OF CAMBERED JOUKOWSKY AIRFOIL, $t/c = 0.15$, $\bar{h}/c = .10$

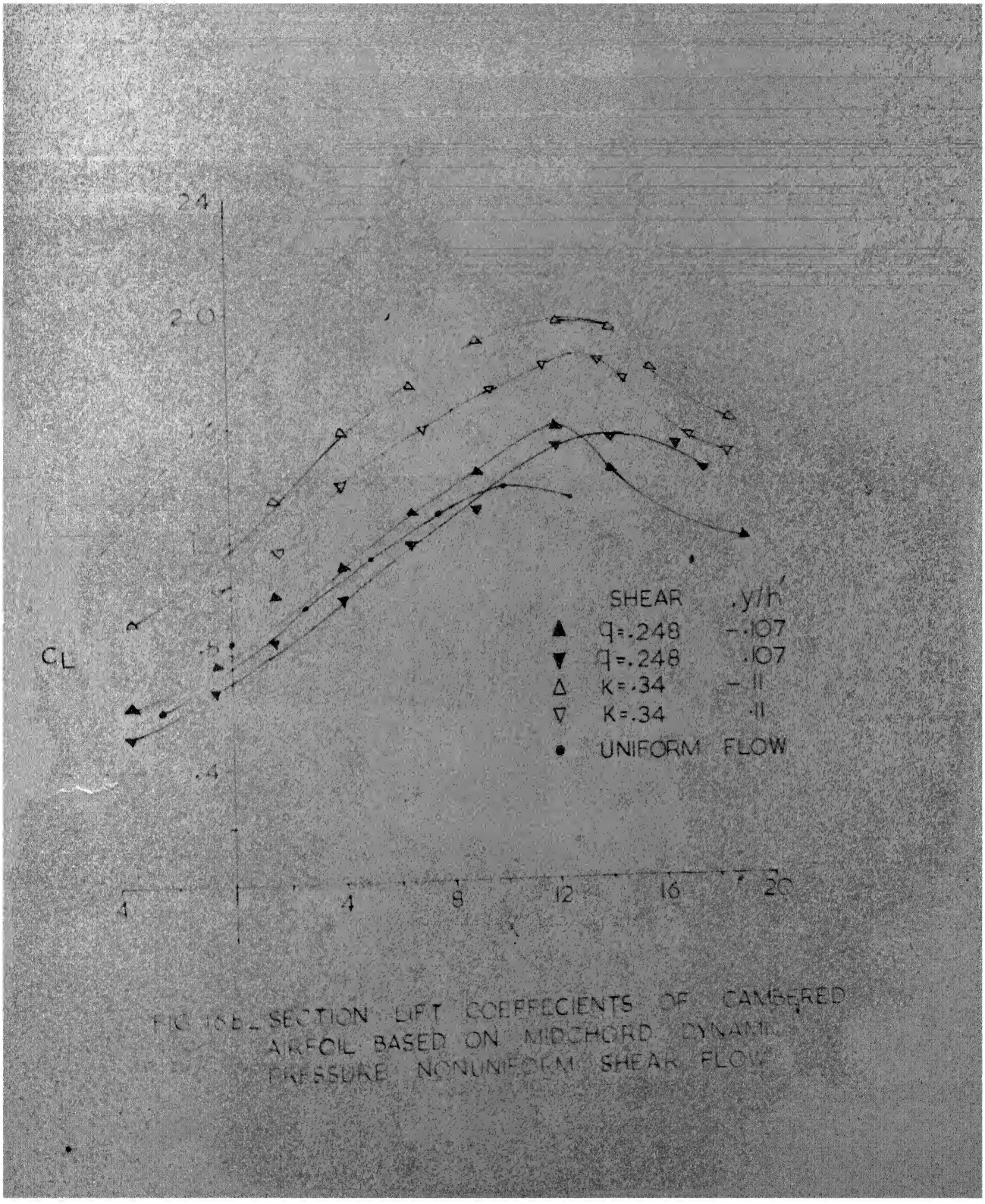

FIG 15b - SECTION LIFT COEFFECIENTS OF CAMBERED AIRFOIL BASED ON MIDCHORD DYNAMIC PRESSURE NONUNIFORM SHEAR FLOW

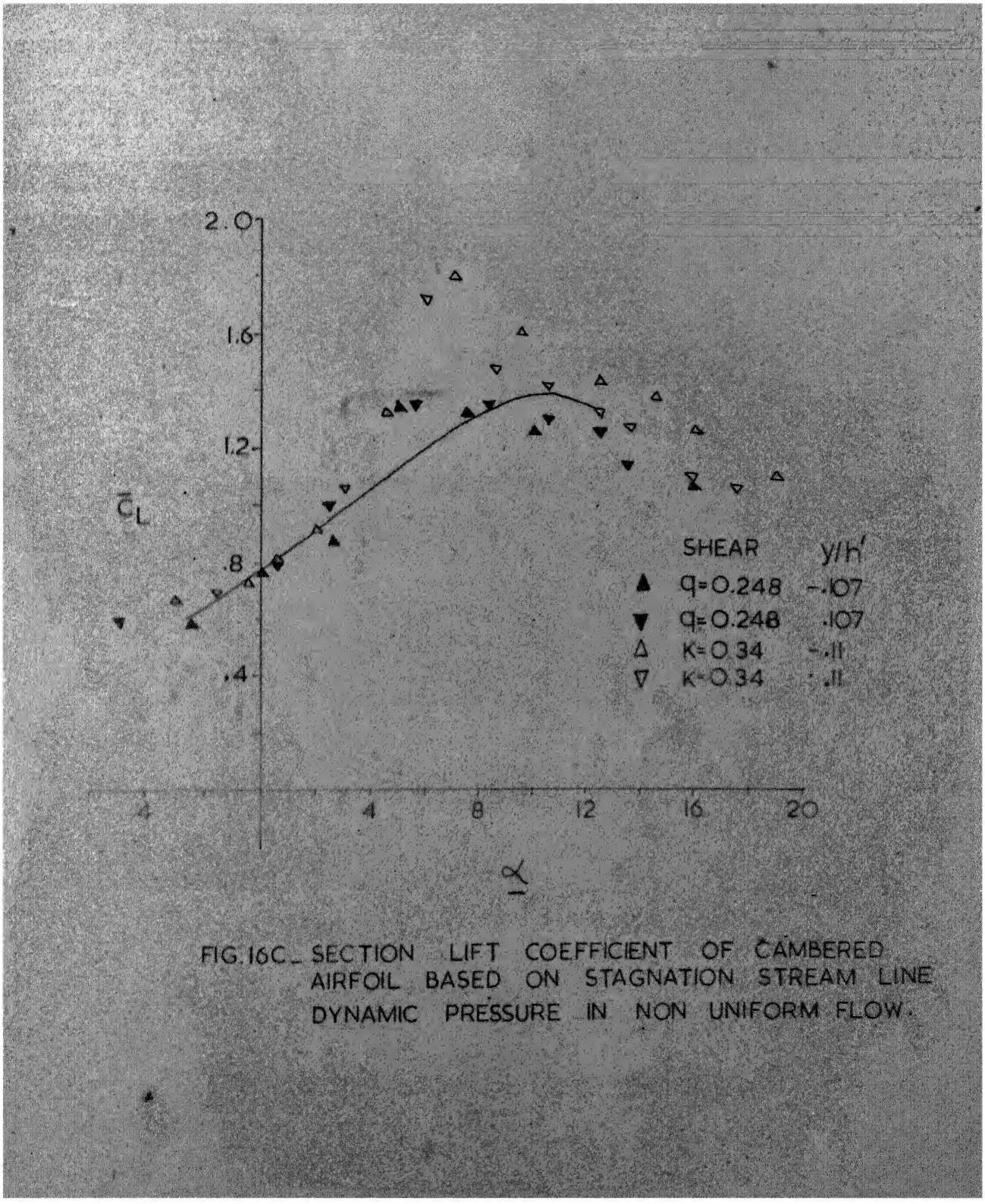

FIG. 16C - SECTION LIFT COEFFICIENT OF CAMBERED AIRFOIL BASED ON STAGNATION STREAM LINE DYNAMIC PRESSURE IN NON UNIFORM FLOW.

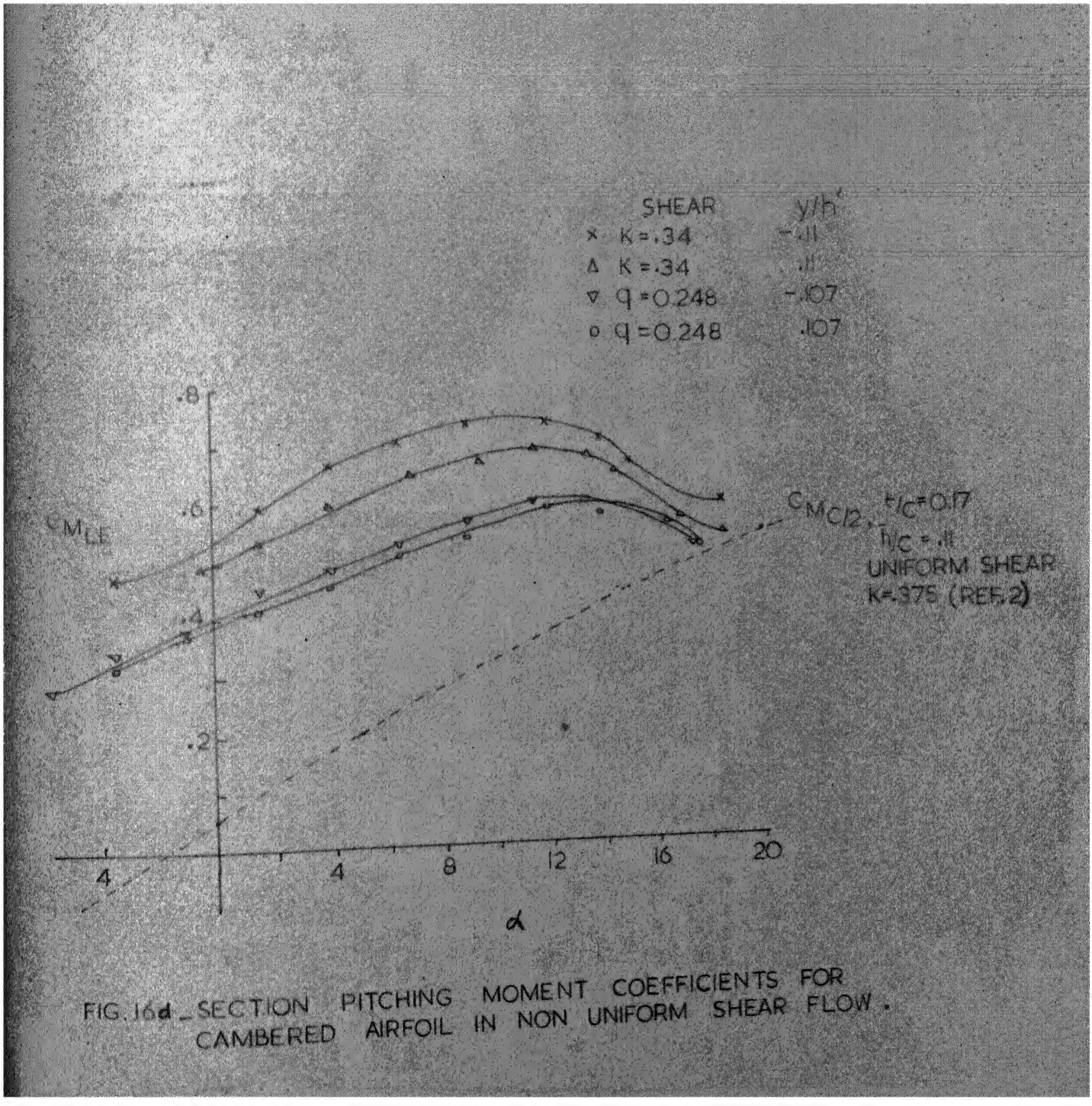

FIG. 16d _ SECTION PITCHING MOMENT COEFFICIENTS FOR CAMBERED AIRFOIL IN NON UNIFORM SHEAR FLOW.

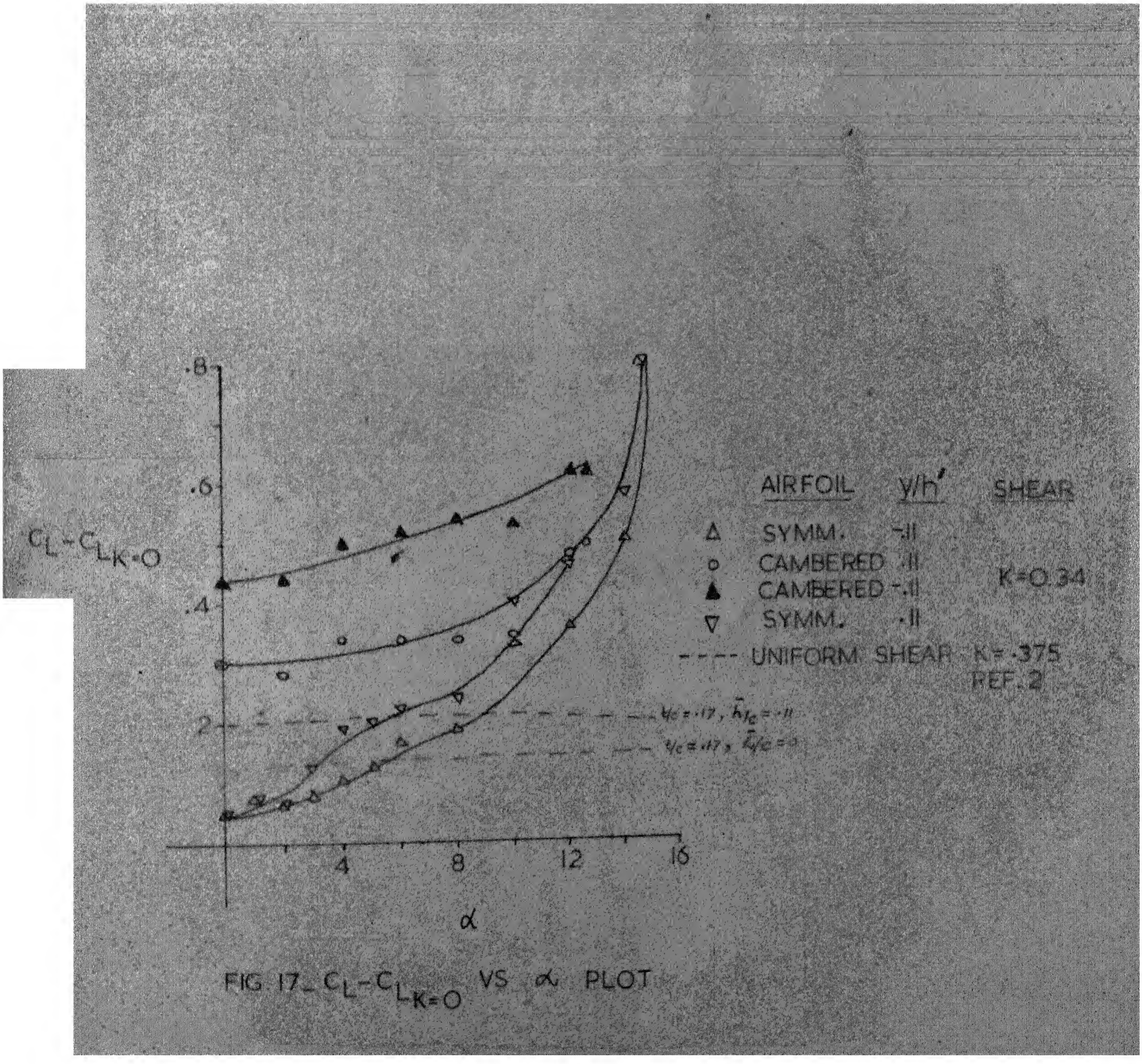

FIG. 17 $C_L - C_{L_{K=0}}$ VS α PLOT

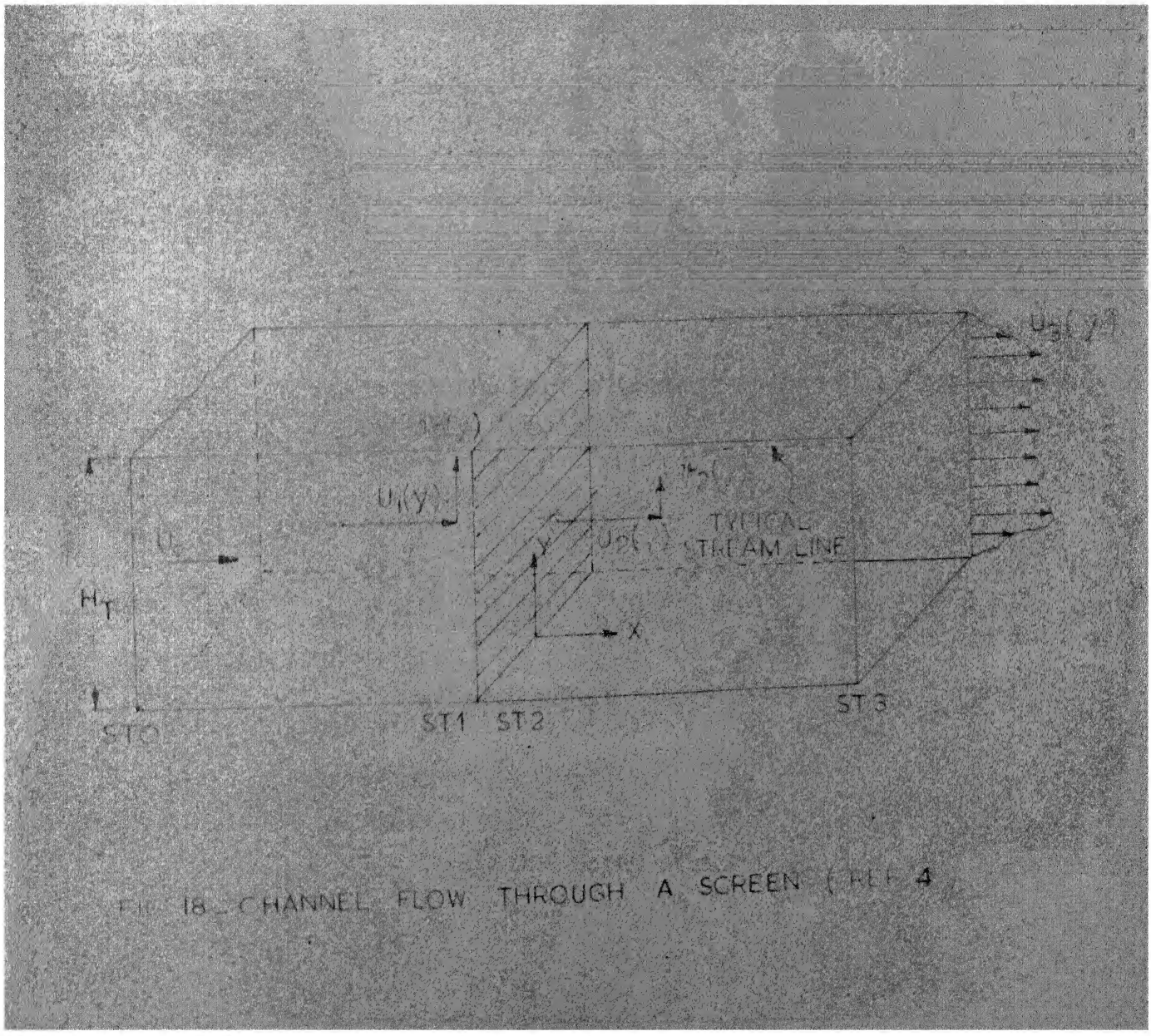

FIG 18 - CHANNEL FLOW THROUGH A SCREEN (REF 4)

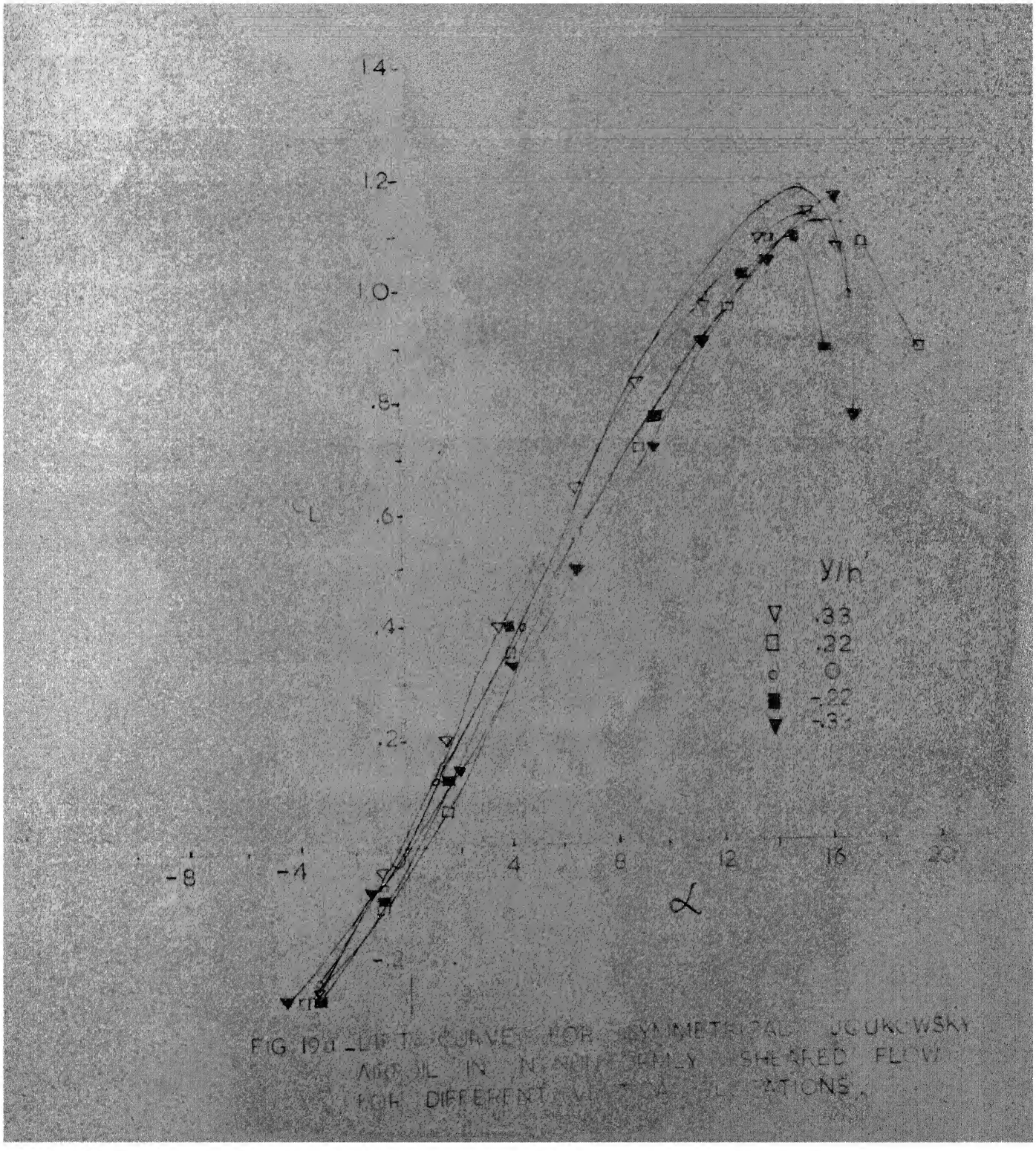

FIG. 19a - LIFT CURVES FOR SYMMETRICAL JOUKOWSKY AIRFOIL IN INFINITE ARRAY OF SHEARED FLOW FOR DIFFERENT VERTICAL LOCATIONS.

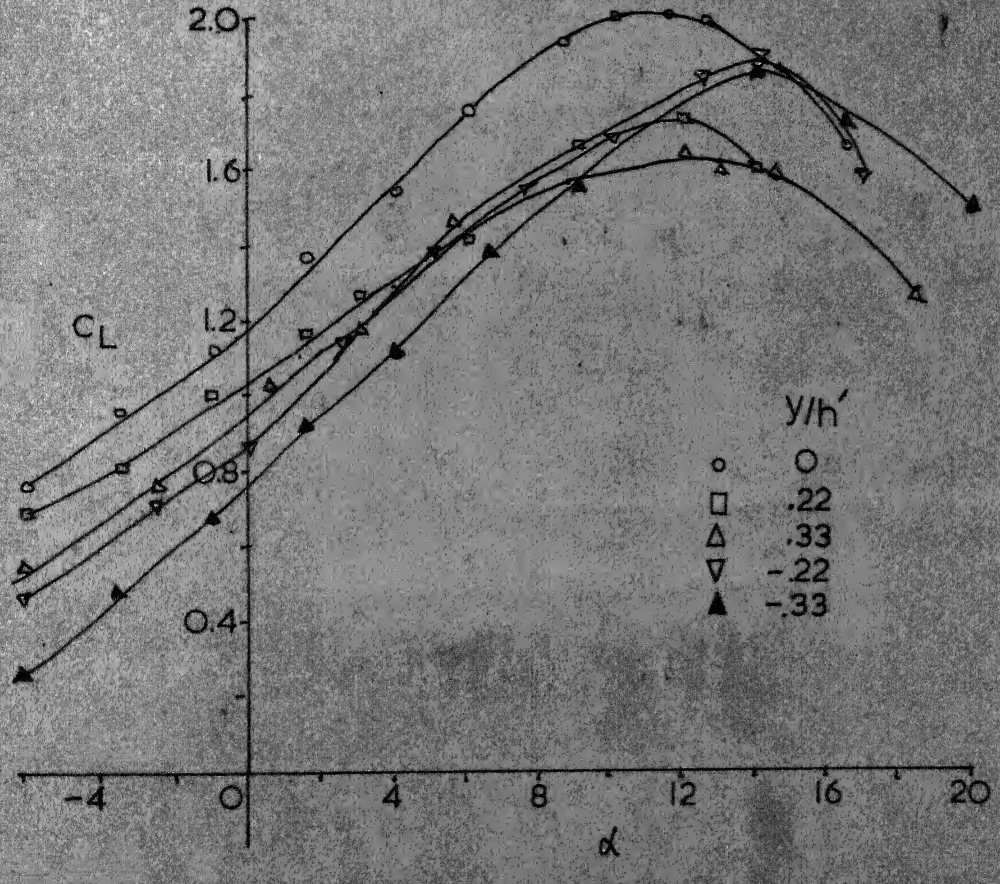

FIG. 19b - LIFT CURVE FOR CAMBERED JOUKOWSKY AIRFOIL IN NONUNIFORMLY SHEARED FLOW FOR DIFFERENT VERTICAL LOCATIONS.

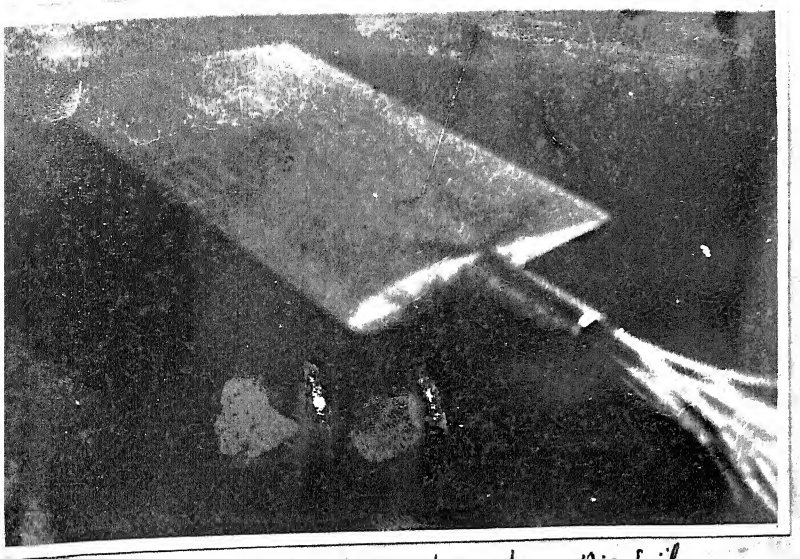

Plate 1a Symmetrical Joukowsky Airfoil

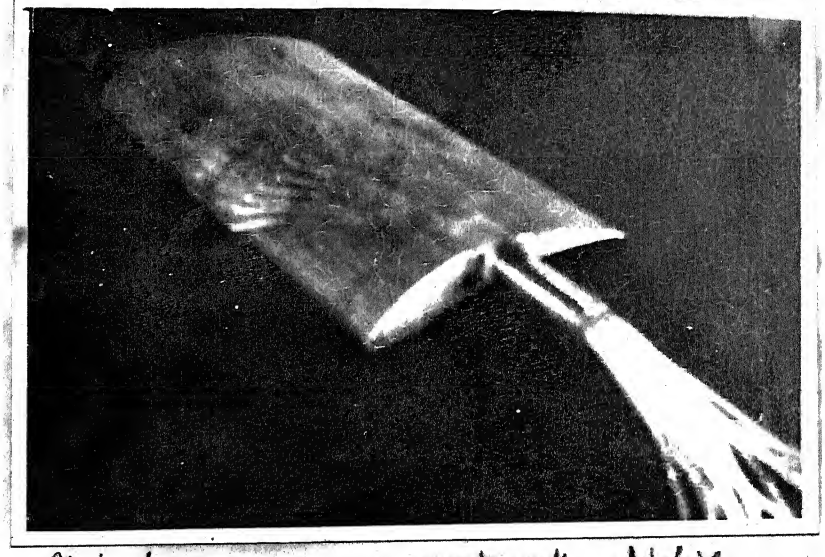

Plate 1b Cambered Joukowsky Airfoil

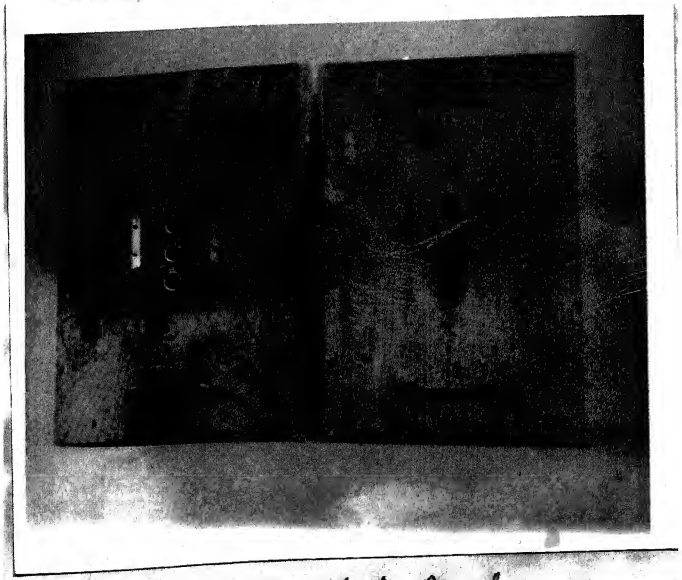

Plate 2 Mounting Panels

Plate 3 Airfoil located at y/c=0

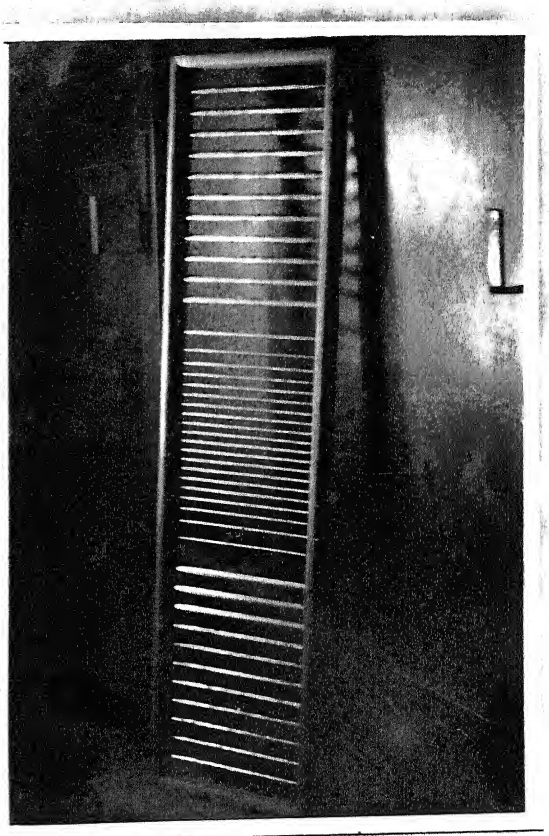

Plate 4a Shear Screen No 1

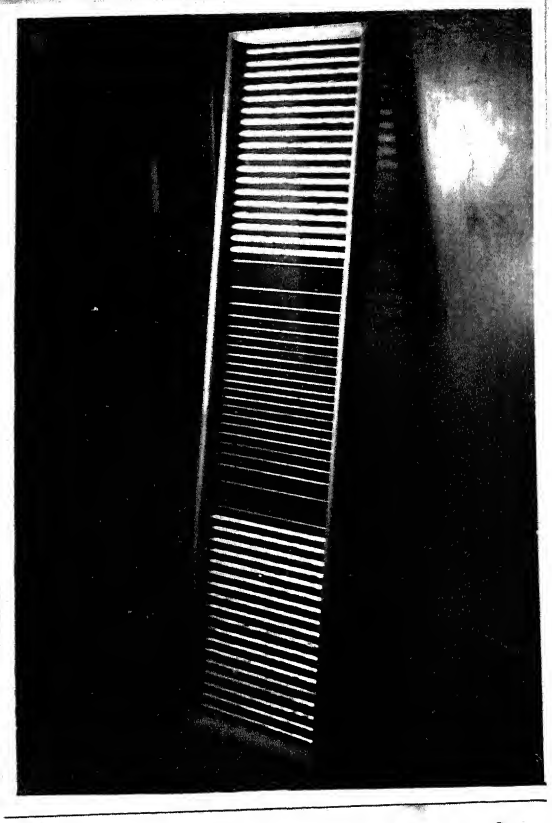

Plate 4b Shear Screen No 2

Plate 5 Shear screen mounted in the test section

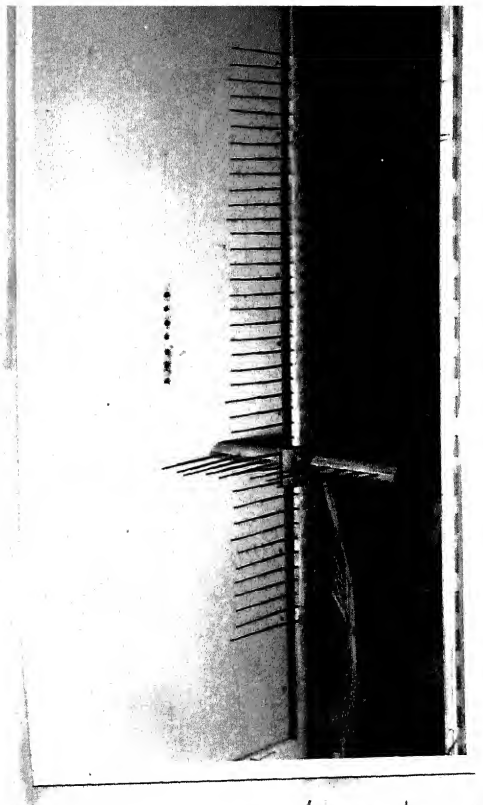

Plate 6 Horizontal rake installation

APPENDIX

A.1 Shear Screen Design

The introduction of the screen in the test-section increases the wind tunnel losses which increase the power factor and accordingly reduces the tunnel efficiency[13]. To avoid this there should be an increase in the tunnel power input. Thus in producing a nomuniform shear flow in a wind tunnel energy is extracted from the stream of air, unlike that in case of slip-stream where energy is imparted to the air by the propeller.

The main limiting factor for the low value of the shear parameter in the present work was the existing horse-power of the blowers, which could not be improved upon.

(i) Design Procedure:

The design procedure given by Vidal et.al[4] is briefly outlined below.

The model used is an initially uniform constant area channel flow (sto) which subsequently passes through a non-uniform screen at st.1 and st.2 and expands to its final con-figuration for a down-stream st. 3.(Fig.18).

The boundary conditions are:

1. The transverse component of the velocity is zero at the wall.
2. The longitudinal velocity component is continuous through the screen.

3. The transverse component changes by a factor β in passing through the screen.
4. On any stream line the change in total pressure between sto and st3 is equal to the local resistance at the point where it is pierced by the stream-line.
5. The static pressure is constant across the channel at st3.

The fluid is assumed to be inviscid and incompressible.

The velocity distribution was represented by a Fourier Series and was subsequently solved by Vidal et.al[4] for the various parameters by applying the boundary conditions. The screen resistance coefficient distribution was obtained across the channel. The spacings and the rod/wire size was decided as explained in 2.1 (iv).

In the present work, condition no.4 was made use of to find out the screen resistance coefficient distribution, from the desired velocity profile with some empirical modifications for the spacings, the final shape was given to the screen no.1. The use of this screen was of interest with a view to study the effect of slip-stream boundaries on airfoil characteristics. The screen no.2 with further modifications (trials and errors) gave a rather satisfactory profile.

Tables A.1 and A.2 give the rod dia-meters and spacings for screen no.1 and screen no.2 (upper half).

TABLE A.1

Rod No.	Distance measured from centre line (cms)
1	0.5
2	2.03
3	3.58
4	5.16
5	6.77
6	8.43
7	10.16
8	12.28
9	15.19
10	20.44
11	23.72

The first nine rods were 1/4" in size. Rods from No.10 onwards were of 1/2" size andwere at a regular interval of 3.28 cms.

TABLE A.2

Rod No.	Distance measured from centre line (cms.)
1	0.5
2	2.03
3	3.58
4	5.16
5	6.77
6	8.43
7	10.16
8	12.28
9	15.19
10	20.82
11	22.82

The first ten rods were of 1/4" in size. Rods from No.11 onwards to No.29 were of 1/2" size and are at regular interval of 2 cms each.

The same size and spacings were used for the lower half in both the screens, for the symmetry of flow about the centre line.

A.2a Joukowsky Airfoils Contours by Conformal Transformation:

The Kutta-Joukowsky transformation produces a family of airfoil shaped curves, having desired thickness and camber. For the two airfoils this transformation was made use of to give the desired shape. The x and y co-ordinates of the curves are given below[16]

$$x = 2b\cos\theta$$

$$y = 2be\,(1+\cos\theta)\sin\theta + 2b\beta\sin^2\theta$$

where $4b$ = chord of the airfoil

e = horizontal shift of transformed circle

and β = twice the percentage camber

with $\beta = 0$, a symmetrical profile is obtained

b = radius of the circle.

A.2b Outlines of the Numerical Integration

$$C_{p_i} = \frac{h_s - h_i}{h_s - h_t} = \frac{p_\infty - p_i}{\frac{1}{2}\rho U_o^2}$$

where h_s, h_t, h_i are the water heads due to static pressure and total pressure of flow and static pressure on model respectively.

$$C_N = \sum_{i=1}^{13} \left\{ (C_{p_{Li}} - C_{p_{Ui}}) + (C_{p_{L_{i+1}}} - C_{p_{U_{i+1}}}) \right\} \left\{ \left(\frac{x}{c}\right)_{i+1} - \left(\frac{x}{c}\right)_i \right\}$$

$$C_{c_u} = \sum_{i=1}^{13} \frac{1}{2} (C_{p_{U_{i+1}}} - C_{p_{U_i}}) \left\{ \left(\frac{y}{c}\right)_{U_{i+1}} - \left(\frac{y}{c}\right)_{U_i} \right\}$$

$$C_{c_L} = \sum_{i=1}^{13} \frac{1}{2} (C_{p_{L_{i+1}}} - C_{p_{L_i}}) \left\{ \left(\frac{y}{c}\right)_{L_{i+1}} - \left(\frac{y}{c}\right)_{L_i} \right\}$$

$$C_c = C_{c_u} + C_{c_L}$$

$$C_M = -\frac{1}{2} \left[\sum_{i=1}^{13} C_{N_i} \left[\left(\frac{x}{c}\right)_{i+1} - \left(\frac{x}{c}\right)_i \right] + \sum_{i=1}^{13} C_{c_{u_i}} \left[\left(\frac{y}{c}\right)_{u_{i+1}} - \left(\frac{y}{c}\right)_{u_i} \right] + \sum_{i=1}^{13} C_{c_{L_i}} \left[\left(\frac{y}{c}\right)_{L_{i+1}} - \left(\frac{y}{c}\right)_i \right] \right]$$

A.2b Turbulence Level Measurements

Following quantities were recorded with the help of DISA Constant Temperature Hot Wire Anemometer.

V_o = Voltmeter reading at zero wind velocity

V = Voltmeter reading at the mean velocity

V_{RMS} = RMS reading in milli volts.

then turbulence level is given by

$$\frac{V_{RMS} \times 4V \times 100}{V^2 - V_o^2}$$